TECHNICAL REPORT R-1

SUPERSONIC FLOW PAST A FAMILY OF BLUNT AXISYMMETRIC BODIES

By MILTON D. VAN DYKE and HELEN D. GORDON

Ames Research Center
Moffett Field, Calif.

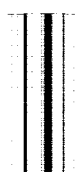

TECHNICAL REPORT R-1

SUPERSONIC FLOW PAST A FAMILY OF BLUNT AXISYMMETRIC BODIES

By MILTON D. VAN DYKE and HELEN D. GORDON

SUMMARY

Some 100 numerical computations have been carried out for unyawed bodies of revolution with detached bow waves. The gas is assumed perfect with $\gamma=5/3$, 7/5, or 1. Free-stream Mach numbers are taken as 1.2, 1.5, 2, 3, 4, 6, 10, and ∞. The results are summarized with emphasis on the sphere and paraboloid.

INTRODUCTION

The problem of supersonic flow past blunt bodies, which has so far largely resisted analytical attacks (ref. 1), has recently yielded to numerical procedures. Of the various schemes that have been proposed (refs. 1 to 6), the simplest is that devised independently in references 1, 3, and 4. It consists in straightforward numerical integration of the equations of motion proceeding downstream from an assumed shock wave.

Various objections can be raised against this procedure, but none has proven fatal. First, the numerical procedure is unstable, in the sense that the inevitable small errors grow geometrically as the solution proceeds. Nevertheless, it can be argued that any given degree of accuracy is attainable in principle, and numerical examples do show that the effect of the instability can be controlled. Second, the method being an inverse one, one must be content with whatever body shapes result. However, shock waves described by conic sections are found to be associated with bodies that are closely described by conic sections, so that one can obtain such bodies of practical interest as the sphere and paraboloid.

These and other aspects of the method have been discussed in reference 1 on the basis of some 50 examples calculated on an electronic computing machine. The purpose of the present paper is to present in greater detail the numerical results for those and additional solutions for axisymmetric bodies at zero angle of attack—a total of some 100 examples.

NUMERICAL PROCEDURE

The numerical method set forth in reference 1 will be summarized here for convenience, and amplified and extended in the light of subsequent experience.

EQUATIONS OF MOTION

Coordinate system.—The detached shock wave is assumed to be described by a conic section so that it is a portion of a hyperboloid of revolution, paraboloid, prolate ellipsoid, sphere, or oblate ellipsoid. In cylindrical polar coordinates originating from its vertex (fig. 1), any such shock is described by

$$r^2=2R_sx-B_sx^2 \tag{1}$$

Here R_s is the nose radius of the shock and B_s, a convenient parameter that characterizes the eccentricity of the conic section, will be called the bluntness. As indicated in figure 2, the bluntness

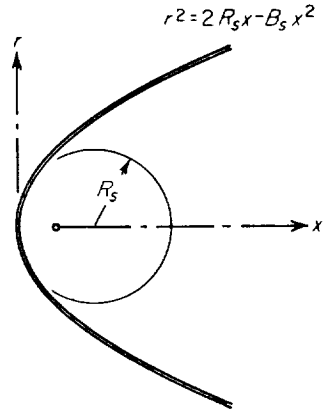

FIGURE 1.—Notation for shock wave.

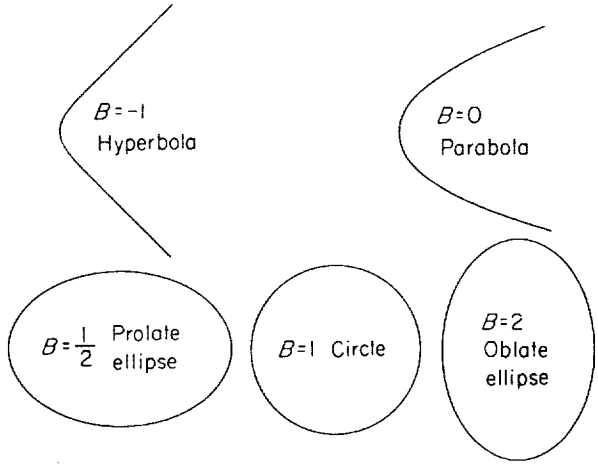

FIGURE 2.—Significance of bluntness B.

is zero for a paraboloid, negative for hyperboloids, positive for ellipsoids, and unity for a sphere.

An orthogonal coordinate system (ξ,η) that contains the shock wave as one of its coordinate surfaces is introduced by setting

$$\frac{x}{R_s}=\frac{1}{B_s}\left[1-\sqrt{(1-B_s\xi^2)(1-B_s+B_s\eta^2)}\right] \quad (2a)$$

$$\frac{r}{R_s}=|\xi|\eta \quad (2b)$$

Special cases are

$$\frac{x}{R_s}=\frac{1}{2}(1+\xi^2-\eta^2) \quad \text{for parabola } (B_s=0) \quad (2c)$$

$$\frac{x}{R_s}=1-\eta\sqrt{1-\xi^2} \quad \text{for circle } (B_s=1) \quad (2d)$$

The shock wave is described by $\eta=1$. For ellipses $(B_s>0)$ this gives only the left half, which is the only part that may form a shock wave. Indeed, except at infinite Mach number, somewhat less than half the ellipse is significant, because the shock degenerates to a Mach wave at

$$\xi^2=\frac{M^2-1}{(M^2-1)B_s+1}$$

This happens also for parabolic and hyperbolic shock waves if $B_s>-(M^2-1)^{-1}$.

For a shock wave no blunter than a sphere (i.e., a hyperboloid, paraboloid, prolate ellipsoid, or sphere), equation (2) describes the entire region of interest. As indicated in figure 3, the upstream axis is described by $\xi=0$ and the downstream axis

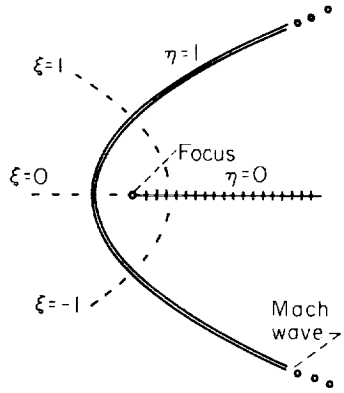

FIGURE 3.—Shock no blunter than a sphere $(B_s\leq 1)$.

by $\eta=0$. A focus lies on the axis at $\xi=\eta=0$; since this singularity cannot lie outside the body, a branch cut can be drawn downstream from it as shown.

For a shock wave blunter than a sphere (oblate ellipsoid) the foci lie off the axis (fig. 4). The flow between and to the right of them is sometimes of interest, but it is not accessible with the present coordinate system. Equation (2a) shows that away from the vertical line joining the foci, variations in x are proportional to the square root of variations in η. This means that the flow quantities, which are presumably analytic functions of the physical coordinates (x,r), will not be analytic in the curvilinear coordinates (ξ,η) in that vicinity. Since the numerical procedure rests on analyticity, it breaks down there. This is of course a purely artificial limitation introduced by

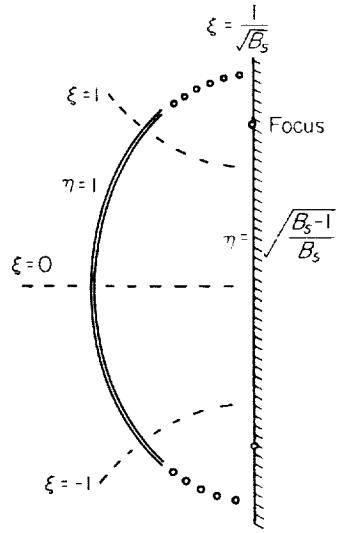

FIGURE 4.—Shock blunter than a sphere $(B_s>1)$.

the coordinates, and could be eliminated by choosing another system.

In this coordinate system, with the azimuthal angle ϕ as the third orthogonal coordinate, the line element ds is given by

$$ds^2=\left(\frac{C\xi^2+\eta^2}{1-B_s\xi^2}\,d\xi^2+\frac{C\xi^2+\eta^2}{C+B_s\eta^2}\,d\eta^2+\nu\xi^2\eta^2d\phi^2\right)R_s^2 \tag{3}$$

where $C\equiv 1-B_s$. Here ν is a parameter that is 0 for plane and 1 for axisymmetric flow, so that both cases can be treated concurrently.

Differential equations and initial conditions.— Let $\vec{V}$ be the velocity referred to the free-stream speed V_∞, ρ the density referred to its free-stream value ρ_∞, and p the pressure referred to $\rho_\infty V_\infty^2$. Then for a perfect gas with constant specific heats the equations of continuity, motion, and energy are, in vector form

$$\operatorname{div}(\rho\vec{V})=0 \tag{4a}$$

$$\rho\,(\vec{V}\cdot\operatorname{grad})\,\vec{V}+\operatorname{grad}p=0 \tag{4b}$$

$$\vec{V}\cdot\operatorname{grad}\,(p/\rho^\gamma)=0 \tag{4c}$$

where γ is the adiabatic exponent.

Then transforming to the (ξ,η) coordinate system with the aid of standard vector relations (and dropping the subscript from B_s for simplicity) gives

$$\left[(\xi\eta)^\nu\sqrt{\frac{C\xi^2+\eta^2}{C+B\eta^2}}\,\rho u\right]_\xi+\left[(\xi\eta)^\nu\sqrt{\frac{C\xi^2+\eta^2}{1-B\xi^2}}\,\rho v\right]_\eta=0 \tag{5a}$$

$$\rho\left[uu_\xi-\frac{C\xi v^2}{C\xi^2+\eta^2}+\sqrt{\frac{C+B\eta^2}{1-B\xi^2}}\,v\left(u_\eta+\frac{\eta u}{C\xi^2+\eta^2}\right)\right]+p_\xi=0 \tag{5b}$$

$$\rho\left[vv_\eta-\frac{\eta u^2}{C\xi^2+\eta^2}+\sqrt{\frac{1-B\xi^2}{C+B\eta^2}}\,u\left(v_\xi+\frac{C\xi v}{C\xi^2+\eta^2}\right)\right]+p_\eta=0 \tag{5c}$$

$$u\sqrt{1-B\xi^2}\,(p/\rho^\gamma)_\xi+v\sqrt{C+B\eta^2}\,(p/\rho^\gamma)_\eta=0 \tag{5d}$$

where u,v are the components of $\vec{V}$ in the ξ,η directions.

The first (continuity) equation is satisfied by introducing a stream function (which is that of Stokes in the axisymmetric case) according to

$$\psi_\eta=(\xi\eta)^\nu\sqrt{\frac{C\xi^2+\eta^2}{C+B\eta^2}}\,\rho u,\qquad \psi_\xi=-(\xi\eta)^\nu\sqrt{\frac{C\xi^2+\eta^2}{1-B\xi^2}}\,\rho v \tag{6}$$

Then the last (energy) equation simply states that

$$p=\rho^\gamma f(\psi) \tag{7}$$

in accord with the fact that entropy is constant along streamlines. Using this to eliminate the pressure from the equations of motion gives

$$\psi_\xi\psi_{\xi\eta}-\psi_\eta\psi_{\xi\xi}-\psi_\xi\left[\psi_\xi\left(\frac{\rho_\eta}{\rho}+\frac{\nu}{\eta}\right)-\psi_\eta\left(\frac{\rho_\xi}{\rho}+\frac{\nu}{\xi}\right)\right]-\frac{\eta}{C\xi^2+\eta^2}\left(\psi_\xi^2+\frac{C+B\eta^2}{1-B\xi^2}\,\psi_\eta^2\right)+\frac{B\xi}{1-B\xi^2}\,\psi_\xi\psi_\eta+(\xi\eta)^{2\nu}\,\frac{C\xi^2+\eta^2}{1-B\xi^2}\,(\gamma\rho^\gamma f\rho_\eta+\rho^{\gamma+1}f'\psi_\eta)=0 \tag{8a}$$

$$\psi_\eta\psi_{\xi\eta}-\psi_\xi\psi_{\eta\eta}+\psi_\eta\left[\psi_\xi\left(\frac{\rho_\eta}{\rho}+\frac{\nu}{\eta}\right)-\psi_\eta\left(\frac{\rho_\xi}{\rho}+\frac{\nu}{\xi}\right)\right]-\frac{C\xi}{C\xi^2+\eta^2}\left(\frac{1-B\xi^2}{C+B\eta^2}\,\psi_\xi^2+\psi_\eta^2\right)-\frac{B\eta}{C+B\eta^2}\,\psi_\xi\psi_\eta+(\xi\eta)^{2\nu}\,\frac{C\xi^2+\eta^2}{C+B\eta^2}\,(\gamma\rho^\gamma f\rho_\xi+\rho^{\gamma+1}f'\psi_\xi)=0 \tag{8b}$$

Values of u,v,p,ρ just behind the shock wave (at $\eta=1$) are found from the oblique shock relations (e.g., ref. 7) in terms of the slope of the bow wave, $\sqrt{1-B\xi^2}/\xi$. Expressed in terms of the stream function, these give the initial conditions

$$\rho=\frac{(\gamma+1)M^2(1-B\xi^2)}{2(1+C\xi^2)+(\gamma-1)M^2(1-B\xi^2)},$$

$$\psi=\frac{\xi^{1+\nu}}{1+\nu},\quad \psi_\eta=\rho\xi^{1+\nu}\text{ at }\eta=1 \tag{9}$$

and for the function $f(\psi)$

$$\left.\begin{aligned} f(\psi)&=\frac{2\gamma M^2(1-Bs^2)-(\gamma-1)(1+Cs^2)}{\gamma(\gamma+1)M^2(1+Cs^2)}\left[\frac{2(1+Cs^2)+(\gamma-1)M^2(1-Bs^2)}{(\gamma+1)M^2(1-Bs^2)}\right]^\gamma\\ s^2&=[(1+\nu)\psi]^{\frac{2}{1+\nu}}\end{aligned}\right\} \tag{10}$$

Form of problem for numerical computation.— For numerical work it is advantageous to use as the independent variable $(1+\nu)\,\psi/\xi^{1+\nu}$, which is constant on the shock and elsewhere more nearly independent of ξ than is ψ, and vanishes only on

the body rather than also on the axis of symmetry. Hence set

$$\psi(\xi,\eta)=\frac{\xi^{1+\nu}}{1+\nu}\,\omega(\xi,\eta) \qquad (11)$$
$$=\frac{1}{2}\,\xi^2\omega(\xi,\eta) \text{ for axisymmetric flow}$$

Then the initial conditions become

$$\rho=\frac{(\gamma+1)M^2(1-B\xi^2)}{2(1+C\xi^2)+(\gamma-1)M^2(1-B\xi^2)},$$
$$\omega=1,\ \omega_\eta=(1+\nu)\rho \text{ at } \eta=1 \qquad (12)$$

and the equations of motion

$$\left[\gamma\left(\rho^{\gamma+1}f\eta^{2\nu}\frac{C\xi^2+\eta^2}{1-B\xi^2}\right)-\left(\omega+\frac{\xi\omega_\xi}{1+\nu}\right)^2\right]\frac{\rho_\eta}{\rho}$$
$$=\frac{\omega_\eta}{1+\nu}\left[\frac{2+\nu}{1+\nu}\,\xi\omega_\xi-\left(\omega+\frac{\xi\omega_\xi}{1+\nu}\right)\left(\frac{B\xi^2}{1-B\xi^2}\right.\right.$$
$$\left.+\frac{\xi\rho_\xi}{\rho}\right)+\left.\frac{\xi^2\omega_{\xi\xi}}{1+\nu}\right]-\left(\omega+\frac{\xi\omega_\xi}{1+\nu}\right)\left(\omega_\eta+\frac{\xi\omega_{\xi\eta}}{1+\nu}\right)$$
$$+\frac{\nu}{\eta}\left(\omega+\frac{\xi\omega_\xi}{1+\nu}\right)^2+\frac{\eta}{C\xi^2+\eta^2}\left[\left(\omega+\frac{\xi\omega_\xi}{1+\nu}\right)^2\right.$$
$$\left.+\frac{C+B\eta^2}{1-B\xi^2}\left(\frac{\xi\omega_\eta}{1+\nu}\right)^2\right]-\left(\rho^{\gamma+1}f\eta^{2\nu}\frac{C\xi^2+\eta^2}{1-B\xi^2}\right)$$
$$\left(\xi^{\nu-1}\frac{f'}{f}\right)\frac{\omega_\eta}{1+\nu}\,\xi^2 \qquad (13a)$$

$$\left(\omega+\frac{\xi\omega_\xi}{1+\nu}\right)\omega_{\eta\eta}=\omega_\eta\left[\frac{\omega_\eta+\xi\omega_{\xi\eta}}{1+\nu}+\left(\omega+\frac{\xi\omega_\xi}{1+\nu}\right)\left(\frac{\rho_\eta}{\rho}\right.\right.$$
$$\left.+\frac{\nu}{\eta}-\frac{B\eta}{C+B\eta^2}\right)-\left.\frac{\omega_\eta}{1+\nu}\,\frac{\xi\rho_\xi}{\rho}\right]$$
$$-\frac{(1+\nu)C}{C\xi^2+\eta^2}\left[\frac{1-B\xi^2}{C+B\eta^2}\left(\omega+\frac{\xi\omega_\xi}{1+\nu}\right)^2+\left(\frac{\xi\omega_\eta}{1+\nu}\right)^2\right]$$
$$+(1+\nu)\rho^{\gamma+1}f\eta^{2\nu}\frac{C\xi^2+\eta^2}{C+B\eta^2}\left[\gamma\,\frac{\rho_\xi}{\xi\rho}\right.$$
$$\left.+\left(\xi^{\nu-1}\frac{f'}{f}\right)\left(\omega+\frac{\xi\omega_\xi}{1+\nu}\right)\right] \qquad (13b)$$

where

$$f=\frac{2\gamma M^2(1-Bs^2)-(\gamma-1)(1+Cs^2)}{\gamma(\gamma+1)M^2(1+Cs^2)}$$
$$\left[\frac{2(1+Cs^2)+(\gamma-1)M^2(1-Bs^2)}{(\gamma+1)M^2(1-Bs^2)}\right]^\gamma, s^2=\xi^2\omega^{\frac{2}{1+\nu}} \qquad (13c)$$

so that

$$\xi^{\nu-1}\frac{f'}{f}=2\omega^{1-\nu}\left[\frac{\gamma B}{1-Bs^2}-\frac{C}{1+Cs^2}\right.$$
$$+\gamma\,\frac{2C-(\gamma-1)M^2B}{2(1+Cs^2)+(\gamma-1)M^2(1-Bs^2)}$$
$$\left.-\frac{2\gamma M^2B+(\gamma-1)C}{2\gamma M^2(1-Bs^2)-(\gamma-1)(1+Cs^2)}\right] \qquad (13d)$$

After these equations have been solved for ρ and ω, the pressure can be found from equation (7), the local Mach number M_l from

$$M_l^2=\frac{2}{\gamma-1}\left[\frac{2+(\gamma-1)M^2}{2\gamma M^2}\,\frac{\rho}{p}-1\right] \qquad (14a)$$

This becomes indeterminate at $\gamma=1$, and one must use instead

$$M_l^2=M_1^2+2ln\,\frac{p_1}{p} \qquad (14b)$$

where

$$p_1=\frac{1-B_s\xi^2\omega}{1+(1-B_s)\xi^2\omega},\quad M_1^2=\frac{M^4p_1(1-p_1)+1}{M^2p_1}$$

The angle θ between the streamline and the axis is given by

$$\theta=\tan^{-1}\sqrt{\frac{1-B_s\xi^2}{1-B_s+B_s\eta^2}}\,\frac{\eta}{\xi}-\tan^{-1}\sqrt{\frac{1-B_s\xi^2}{1-B_s+B_s\eta^2}}\,\frac{\psi_\xi}{\psi_\eta} \qquad (15)$$

NUMERICAL SOLUTION OF THE EQUATIONS

The initial value problem represented by equations (12) and (13) has been solved numerically by forward (i.e., downstream) integration from the shock wave ($\eta=1$) toward smaller values of η. The procedure is indicated schematically in figure 5.

Finite-difference scheme.—Over each interval $\Delta\eta$, the dependent variables ρ and ω_η are extrapolated linearly. Then at each new value of η the ξ derivatives are evaluated by 11-point numerical differentiation (ref. 8). In this process central difference formulae can be used near the axis by taking advantage of symmetry in ξ, and elsewhere except at the largest 5 values of ξ where successively more noncentral formulae are required. The procedure may be summarized as follows:

0. Calculate initial values at $\eta=1$ from equation (12).

1. Calculate ξ derivatives $\rho_\xi, \omega_\xi, \omega_{\xi\xi}, \omega_{\xi\eta}$ by 11-point numerical differentiation.

2a. Calculate ρ_η from equation (13a).

2b. Calculate $\omega_{\eta\eta}$ from equation (13b).

3a. Extrapolate ρ and ω_η linearly to next smaller value of η:

$$\rho^{(m+1)}=\rho^{(m)}-(\Delta\eta)\rho_\eta^{(m)},\omega_\eta^{(m+1)}=\omega_\eta^{(m)}-(\Delta\eta)\omega_{\eta\eta}^{(m)} \tag{16a}$$

3b. Extrapolate ω using averaged value of ω_η:

$$\omega^{(m+1)}=\omega^{(m)}-\tfrac{1}{2}(\Delta\eta)[\omega_\eta^{(m)}+\omega_\eta^{(m+1)}] \tag{16b}$$

4. Repeat steps 1 to 3b at this new value of η, and continue until ω is entirely negative at all N points.

The surface of the body is then found on each line ξ=const. as the point at which ω vanishes according to equation (16b). This is at $\eta=\eta^{(p)}-\delta\eta$ where

$$\delta\eta=\frac{\omega_\eta^{(p)}-\sqrt{\omega_\eta^{(p)2}-2\omega^{(p)}\omega_{\eta\eta}^{(p)}}}{\omega_{\eta\eta}^{(p)}} \tag{16c}$$

if ω becomes negative after the pth point.

External iteration on ρ.—After completion of the integration, the accuracy of ρ (and hence of p) can be greatly increased by recomputing it using the averaged values of ρ_η over each interval $\Delta\eta$, so that the revised value after the mth step is given by

$$\rho^{(m)}=\rho^{(0)}-(\Delta\eta)[\tfrac{1}{2}\rho_\eta^{(0)}+\rho_\eta^{(1)}+\rho_\eta^{(2)}+\cdots+\rho_\eta^{(m-1)}+\tfrac{1}{2}\rho_\eta^{(m)}] \tag{17}$$

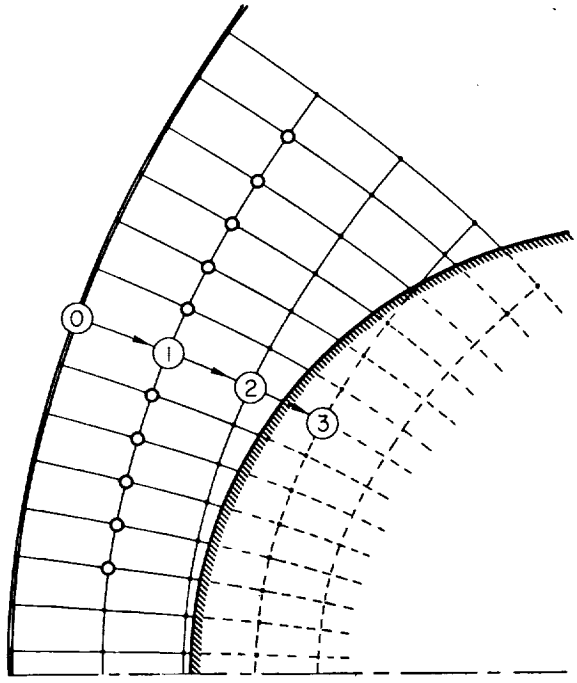

FIGURE 5.—Finite-difference scheme.

Figure 6 shows how in a typical case the accuracy is thus improved by at least an order of magnitude. The virtue of this "external iteration" is that just like conventional iteration it reduces the error in ρ (and p) from $0(\Delta\eta)^2$ to $0(\Delta\eta)^3$, but the computing time is almost unchanged rather than doubled.

Instability.—The numerical procedure is unstable in the region of subsonic flow. However, the effect on the solution is altogether negligible except at Mach numbers very close to unity. An

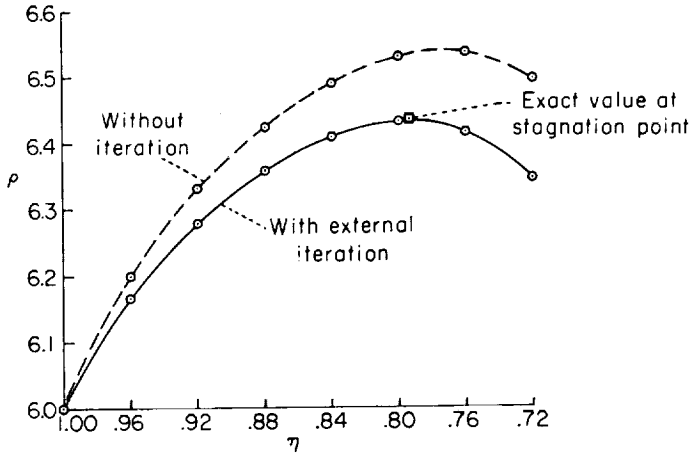

FIGURE 6.—Density on axis behind parabolic shock wave at $M=\infty$, $\gamma=7/5$.

example in reference 1 showed that at $M=\infty$ the round-off errors are amplified by the instability so as to invalidate the last two significant figures if one takes 11 steps between the shock and the nose of the body, the last 4 figures if one takes 15 steps, and so on. However, 5 or 6 steps are found to give the flow quantities of interest accurate to within 1 percent. Hence, the instability is of no practical concern.

The instability becomes discernible only when the free-stream Mach number is reduced to something like 1.2. Then the derivative $\omega_{\eta\eta}$ displays appreciable oscillations just ahead of the stagnation point, as shown in figure 7. The nose of the body is corrugated as a consequence. However, the effect is still so small that the corrugations have been magnified fortyfold in figure 8 to make them visible. In any case, it is a virtue of the instability that the errors oscillate (rather than, say, varying exponentially) in the vertical direction, so that they can never go undetected.

Convergence, existence, and uniqueness.—It seems certain that the numerical procedure, though unstable, converges in the sense that the error can be reduced below any preassigned small limit. (To increase the accuracy one must work with more significant figures, but this is true also of stable schemes.) Apparent convergence was demonstrated experimentally in reference 1, both internally by refining the mesh size and externally by comparing with the method of Garabedian and Lieberstein (ref. 6), for which convergence has been rigorously proved.

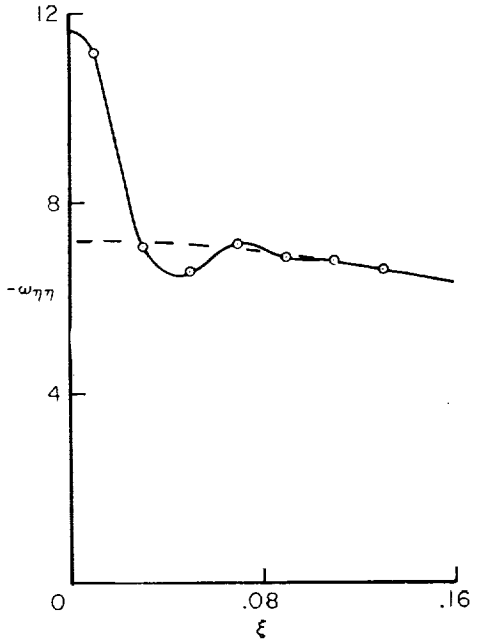

FIGURE 7. Effect of instability on $\omega_{\eta\eta}$, case 139, $\eta=0.76$.

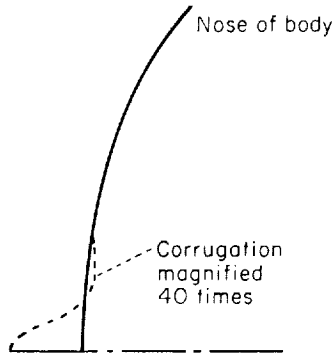

FIGURE 8.—Effect of instability on nose shape, case 139.

The difference scheme used for the η integration is the simplest possible one (except for the external iteration). The truncation error could be reduced by iterating each step, but because the procedure is unstable the round-off error would be greatly increased. Whether a net gain would result is probably best determined by trial. (Iteration was attempted at an early stage in the present investigation, and found to be disastrous. However, this is now believed to have resulted from the division by zero in calculating ρ_η/ρ that is discussed in the next section.)

It may appear inconsistent to combine such a crude scheme for the η integration with an 11-point difference formula for the ξ derivatives. The purpose was to make the error associated with $\Delta\xi$ negligibly small, and thus simplify consideration of the truncation error by effectively reducing it to a function of $\Delta\eta$ alone. Trial has shown in one case that the accuracy is unaffected by using a 7-point formula instead, but definitely deteriorates with a 3-point formula.

Detached shock waves seem always to be smoother than the body that produces them. Hence it is fair to conjecture that an analytic body produces an analytic shock. Conversely, an analytic shock wave undoubtedly leads to a body that is analytic if it exists at all. However, it is not clear that a real body will always exist. For example, applying the present procedure to the wiggly shock wave of figure 9 might lead to singularities before a body is reached, or to a number of small bodies. Fortunately, the family of

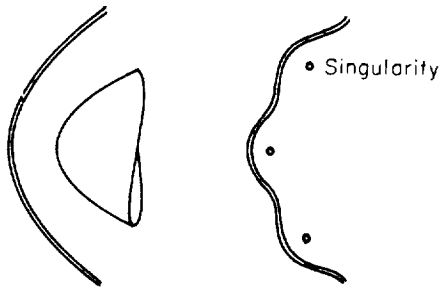

FIGURE 9.—Analytic shock waves that do and do not produce single bodies.

conic-section shock waves appears to be sufficiently smooth that it always leads to a single body.

Experience suggests that if a body exists for a prescribed shock wave, its shape is uniquely determined. It is true that, particularly at high Mach numbers, the shock shape varies only slightly with changes in body shape. However, this remaining dependence is readily determined with the present numerical method. (See ref. 1.)

Program for electronic computer.—This procedure has been programed for machine computation on the IBM 650 electronic digital computer with floating decimal attachment. For each value of η the flow quantities are calculated at the N equally spaced values $\xi=(n-\frac{1}{2})(\Delta\xi)$, $1\leq n\leq N$, where N may have any prescribed value between 11 and 50. These straddle the axis of symmetry (fig. 5) in order to avoid the indeterminate form ρ_ξ/ρ in equation (13b) (which would otherwise require the evaluation of $\rho_{\xi\xi}$ on the axis and the use of L'Hospital's rule). The mesh dimensions ($\Delta\xi$) and ($\Delta\eta$) are arbitrary (but equal for all steps).

Provision has also been made for dropping five of the outermost points at each step in η. Dropping five points means that only central-difference formulae are being used. The equations actually programed embrace plane as well as axisymmetric flow (ref. 1). Thus the parameters that are prescribed, and their ranges, are

M	free-stream Mach number	$1<M<\infty$
B_s	bluntness of conic section describing shock wave	$-\infty<B_s<\infty$
ν	0 for plane, 1 for axisymmetric flow	
γ	adiabatic exponent	$1\leq\gamma$
$\Delta\xi,\Delta\eta$	mesh dimensions	$0<\Delta\xi,\Delta\eta$
N	number of points on shock wave	$11\leq N\leq 50$
c	number of end points dropped per step	$c=0$ or 5

708307 O - 61 - 2

The machine is programed to stop when ω becomes negative at the outermost point, which ordinarily means that the entire computation has reached the interior of the body.

Machine computing time is 1¼ minutes per value of η if 20 points are taken on the shock wave and none dropped. Four to eight steps in η yield ample accuracy, so that a typical case requires 5 to 10 minutes computing time.

The flow variables that are ordinarily printed for each mesh point are

ω, ω_ξ, ω_η, $\omega_{\eta\eta}$

ρ (externally iterated), ρ_η (not iterated)

p (calculated from externally iterated ρ)

$$D=\left[\gamma\left(\rho^{\gamma+1}f\eta^{2\nu}\frac{(\xi^2+\eta^2)}{1-B\xi^2}\right)-\left(\omega+\frac{\xi\omega_\xi}{1+\nu}\right)^2\right]$$

M_l

As discussed in the next section, the quantity D, which is seen from equation (13a) to be the denominator in the computation of ρ_η, is printed to determine whether it becomes negative.

Table I shows the printed results for a sphere at infinite Mach number with $\gamma=1.4$. For brevity, only alternate (even-numbered) values of ξ have been included.

LIMITATIONS ON SOLUTIONS

In the example of table I, the computation terminated as planned, ω having become entirely negative at the last value of η. Unfortunately, this conclusion is not invariably reached. There are several shortcomings in the procedure which may prematurely stop the computation, and these limit the extent to which the solution can be carried downstream. These and other difficulties with the program will be described here.

Division by zero in computing ρ_η/ρ.—The coefficient of ρ_η/ρ in equation (13a), already denoted by D, vanishes along a line that runs downstream from the body to the shock in the supersonic region, as illustrated in figure 10. The right-hand side of equation (13a) should also vanish there, so that ρ_η/ρ is regular. However, in a numerical solution the numerator and denominator do not vanish on precisely the same line, and the resulting singularity produces wild fluctuations that shortly lead to a negative value of ρ and thereby stop the solution.

No way of overcoming this difficulty has been

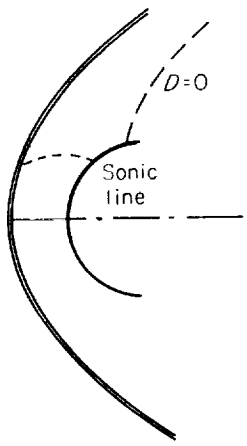

FIGURE 10.—Form of line where $D=0$.

found, and the solution must accordingly be restricted to the region where D is positive. It is for this purpose that D appears in the printed results (cf. table I). Fortunately, the surface Mach number reaches 1.3 or 1.5 in that region, so that the solution extends well beyond the sonic line adequate for continuing the solution by the method of characteristics.

Using a similar numerical procedure, Mangler has calculated a single example, that of plane flow past a circle at $M=7$ with $\gamma=1.4$ (ref. 3). He finds that the accuracy becomes insufficient somewhat behind the sonic line. If this is evidence of the difficulty under discussion, his example would suggest that it will not necessarily be eliminated by a transformation of variables, since his are entirely different. It would be helpful to determine whether the line $D=0$ has any simple physical significance.

Division by zero in computing $\omega_{\eta\eta}$.—A second imperfection appears when the factor $[\omega+\xi\omega_\xi/(1+\nu)]$ in equation (13b) vanishes, leading to a singularity in $\omega_{\eta\eta}$. This can happen only inside the body (for $\omega<0$), so that the effect is usually not serious, but it sometimes stops the calculation prematurely by one step. This difficulty could be eliminated by re-programing so that all points that fall inside the body are deleted from the computation (which would require the use of noncentral differentiation formulae near the axis).

End instability.—At the outermost 5 values of ξ, progressively more noncentral formulae are used for the numerical differentiation. These involve small differences of large numbers, and so produce instability even in the region of supersonic flow. In reference 1, all limitations on the downstream extent of the calculation were attributed to this "end instability." However, the more flexible present program permits the end instability to be eliminated by dropping the outermost 5 points at each step. Thus it has been found that end instability is almost as harmless as the conventional numerical instability, and that the two types of division by zero just discussed are the principal causes of premature stopping of the computation. However, the oscillations resulting from division by zero near the axis (in the second case) may, because of the end instability, induce oscillations at the outermost points which stop the computation there. Fortunately, this ordinarily occurs only after the surface of the body has been reached over the whole range of ξ. Otherwise, end instability usually does no more than make the outermost 2 or 3 points erratic near the body surface.

Unattainability of very blunt bodies.—Flat-nosed bodies cannot be treated with the present coordinate system. They lie downstream of the foci (fig. 4), a region into which the present scheme cannot penetrate. Ahead of that region the method gives every indication of converging. Hence to treat very blunt bodies (such as flat-nosed ones) it would merely be necessary to substitute a coordinate system that is analytic past the foci. A suitable choice is the nonorthogonal "sheared Cartesian" system (z,r) illustrated in figure 11.

Nose corrugation.—Most of the solutions were carried out with $N=20$, giving some 15 points on the body between the stagnation point and the sonic line. This spacing is much closer than required for accuracy, and at low Mach numbers may unnecessarily accentuate the nose corrugation indicated in figure 8. This difficulty can be minimized by choosing $\Delta\xi$ no smaller than 0.02 at Mach numbers near 1.

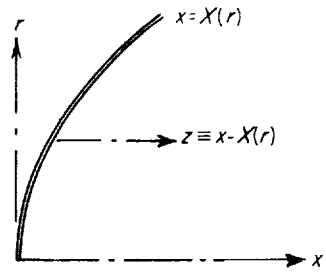

FIGURE 11.—Sheared Cartesian coordinate system.

Other limitations.—There are two other limitations to be remembered. First, if $B_s > -(M^2-1)^{-1}$, the range of ξ must not extend to the point where the shock wave degenerates to a Mach wave, at

$$\xi^2=\frac{M^2-1}{(M^2-1)B_s+1}$$

Violating this restriction leads to a division by zero which promptly stops the computer. Second, with the 11-point differentiation scheme of the present program, the computation stops if the number of points at any value of n (which is N if no end points are dropped) falls below 11.

The choice of interval sizes $(\Delta\xi,\Delta\eta)$, and of the number of points depends on the stand-off distance and the extent of the subsonic flow region. To facilitate the choice, the values of η at the nose of the body, η_o, and of ξ at the sonic point on the body, ξ_*, are shown in figure 12 for the sphere and paraboloid.

REDUCTION OF DATA

The shape of the body and sonic line were found by hand computation from the machine results exemplified by table I. (Had a larger computer been available, this work would also have been done by the machine.)

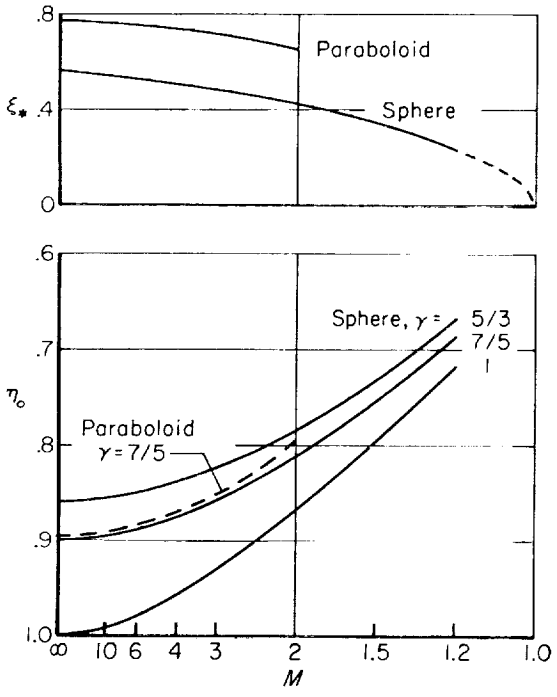

FIGURE 12.—Coordinates of sonic point and of nose for sphere and paraboloid.

Determination of body and sonic line.—At each value of ξ the value of η at the body surface is given by equation (16c). Then equations (2) give the Cartesian coordinates of body points. The surface pressure was found by extrapolation to the same value of η using the values of pressure at the last three points outside the body; that is

$$p_b=p^{(p-1)}-\frac{1}{2}\left(\frac{\delta\eta}{\Delta\eta}\right)[p^{(p)}-p^{(p-2)}]$$
$$-\frac{1}{2}\left(\frac{\delta\eta}{\Delta\eta}\right)^2[2p^{(p-1)}-p^{(p)}-p^{(p-2)}] \quad (18)$$

if ω becomes negative after the pth point for a given value of ξ.

Values at the outermost points $(n=N)$ were invariably discarded because of the end instability, and their neighbors were also regarded with suspicion and rejected in case of doubt.

Values of η_b and p on the axis of symmetry were obtained by extrapolation from the first and second points $(n=1,2)$ according to

$$^{(0)}p=\frac{9}{8}\,^{(1)}p-\frac{1}{8}\,^{(2)}p \quad (19)$$

Points on the sonic line were calculated simply by interpolating linearly (with respect to η at a given ξ) in the local Mach number.

Approximation of body by conic section.—The bodies are found to be described by simple smooth (undoubtedly analytic) curves. They can invariably be closely approximated by conic sections back to the sonic point (or, what is practically the same thing, back to the limiting characteristic beyond which changes in body shape do not affect the subsonic flow field). Thus, corresponding to equation (1), the body is approximated by

$$r^2=2R_b(x-\Delta)-B_b(x-\Delta)^2 \quad (20)$$

where Δ is the stand-off distance, R_b the nose radius of the body, and B_b its bluntness (cf. fig. 2). The fit was made by plotting $r^2/2(x-\Delta)$ as a function of $(x-\Delta)$ for the computed body points, and simply estimating the best straight-line approximation back to the sonic point. The shapes are so close to conic sections that no greater care is necessary. Thus, in the example of table I the body is approximated by a sphere of radius $R_b/R_s=0.7662$ with center at $x/R_s=0.8645$, and the actual computed body points (table IV, case

180) deviate from that sphere by less than 1 part in 1000 back to somewhat beyond the sonic point. Shortly thereafter, however, the shape begins to differ significantly from a conic section.

RESULTS OF CALCULATIONS

SURVEY OF BODY SHAPES

The first stage in the investigation was a systematic survey of the family of axisymmetric bodies. The effects of varying both shock shape and free-stream Mach number were explored for $\gamma=7/5$ and, to a lesser extent, for $\gamma=1$ and 5/3 (which are the possible extremes for a gas).

Tabulation of solutions.—Table II summarizes 80 solutions for axisymmetric flow. The present survey began with case 86, but a number of earlier solutions at various Mach numbers, including those used in reference 1, are also given. The number of steps taken on the axis between the shock wave and body is shown as a measure of accuracy, five or more steps generally assuring an accuracy of less than 1 percent in all physical quantities of interest. The original case numbers have been retained to avoid confusion. Gaps in numbering correspond to solutions for plane flow, abortive attempts, or cases of little interest (such as repetitions, coarser meshes, etc.).

Dependence of body shape.—Figure 13(a) shows the variation of body shape (as measured by its bluntness) with shock-wave shape for $\gamma=7/5$ at the standard free-stream Mach numbers of 1.2, 1.5, 2, 3, 4, 6, 10, and ∞. (Solutions for $M=\infty$ were actually computed with $M=10{,}000$.) The range is sufficient to encompass the sphere ($B_b=1$) and the paraboloid ($B_b=0$) except at low Mach numbers. Similar surveys for $\gamma=1$ and $\gamma=5/3$ were restricted to the neighborhood of the sphere, as shown in figures 13(b) and 13(c). The slopes through points for $B_b=1.0$ were estimated by comparison with figure 13(a).

By interpolating in the results of the survey (figs. 13), one can determine with good accuracy the shock wave that leads to a desired conic-section body at a given Mach number. The sphere (or hemisphere) is a convenient standard shape for either wind-tunnel or free-flight testing, so that the greatest amount of experimental data has accumulated for it. Consequently, the sphere has been chosen as one of two shapes to be investigated in detail here, and it alone has been studied at values of γ different from 7/5.

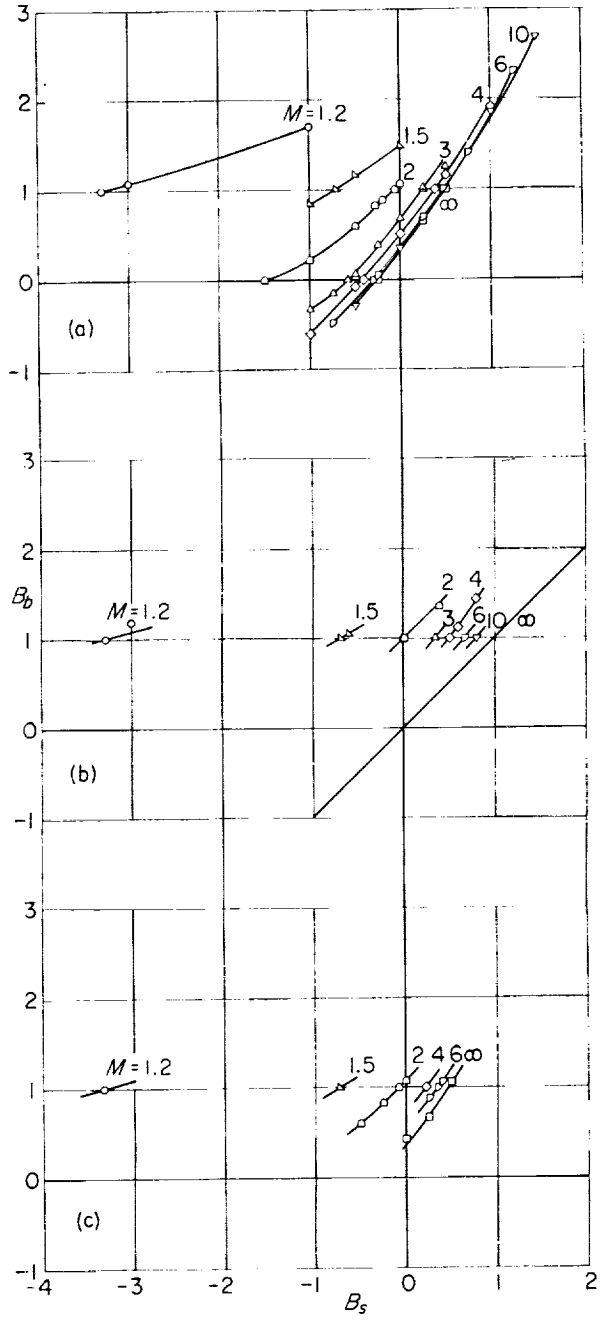

(a) $\gamma=7/5$ (b) $\gamma=1$ (c) $\gamma=5/3$

FIGURE 13.—Relation between shock wave and body shapes.

Figure 14 shows the variation with Mach number of the shock-wave shape for a sphere with $\gamma=1$, 7/5, and 5/3, and for a paraboloid with $\gamma=7/5$. At high Mach numbers the variation with γ is seen to be greatest for γ near 1.

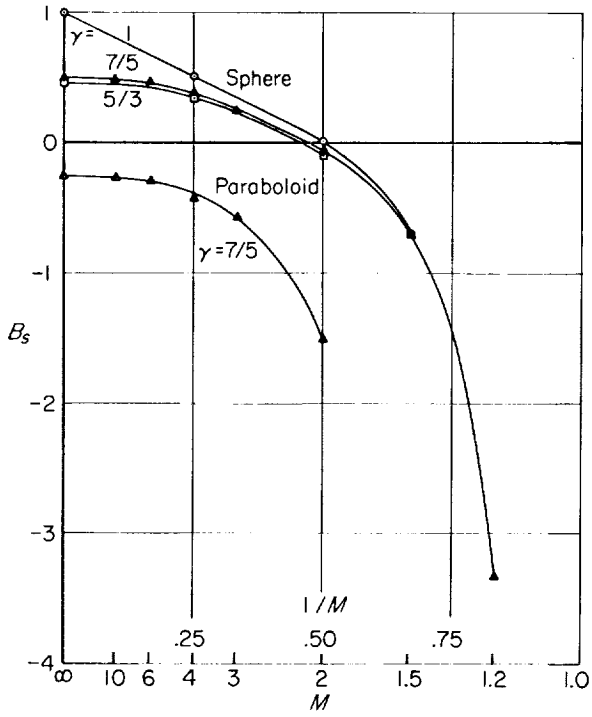

FIGURE 14.—Shock wave bluntness for sphere and paraboloid.

SOLUTIONS FOR SPHERES AND PARABOLOIDS

On the basis of the survey, final solutions were run for the sphere with $\gamma=1$, 7/5, and 5/3, and the paraboloid with $\gamma=7/5$. The initial data and various geometrical ratios for the resulting body are summarized in table III.

Table IV gives for each of these 29 cases the shapes of the body, shock wave, and sonic line (all expressed in Cartesian coordinates with origin at the shock vertex and initial shock radius of curvature as unit of length) and the surface pressure (referred to $\rho_\infty V_\infty^2$). The exact value of pressure at the stagnation point is also listed as a criterion of accuracy. For brevity, results are given only for alternate points (even values of n).

Figures 15(a) to 15(d) show the variation with Mach number of the shock wave and sonic line. (Here the origin is at the center of curvature of the body, and its radius is the unit of length.) No attempt has been made to fair the sonic lines into the shock wave with the slope which can, with some effort, be computed exactly (ref. 9). Figure 15(e) shows the slight movement of the sonic line as γ is varied at a Mach number of 1.2. The computed points are shown as an indication of the consistency of the results.

DISCUSSION OF RESULTS

Shape of sonic line.—Several investigators have recently discussed the shape of the sonic line, in particular as it issues from the surface of the body. In plane flow it must always lean downstream as it emerges. In axisymmetric flow, however, Probstein has pointed out (ref. 10) that it may lean upstream at sufficiently high Mach numbers, and has suggested that the change will occur at about $M=3$ for a sphere in air. Figure 15(a) confirms his qualitative conclusions, and shows that the change occurs near $M=4$. The significance of this change is that at higher speeds, changes in body shape in the supersonic region do not affect the subsonic flow region.

Figure 15(d) shows that for spheres in monatomic gas the change never occurs. On the other hand, figure 15(b) shows that it has already occurred at $M=2$ for a paraboloid in air.

Stand-off distance.—The distance Δ between the shock and the body on the axis of symmetry is an easily measured quantity that has recently been employed as measure of real gas effects (e.g., ref. 11). The variation of this quantity with Mach number is shown in figure 16(a). Comparison with experiment is shown for diatomic gases [1] ($\gamma=7/5$) in figure 16(b), and for monatomic gases ($\gamma=5/3$) in figure 16(c).

Various students of hypersonic flow have suggested that the stand-off distance should depend only on the density ratio across a normal shock wave. The extent to which this is true is shown in figures 17(a) and 17(b) by correlating on that basis the present solutions for different body shapes and values of γ. The result of Lighthill's incompressible approximation is shown for comparison (ref. 12). The correlation seen in figures 17 serves as a check of the over-all consistency of the numerical solutions. It also suggests that interpolation for stand-off distance at other values of γ should be carried out on the basis of figure 17(a).

Surface pressures.—The solutions with $\gamma=1$ do not include $M=\infty$ because that is a degenerate case in which the shock wave and body coalesce, with finite pressure changes occurring in the intervening infinitesimal layer. In that limit the flow field is given analytically by the "Newtonian plus centrifugal" theory of Busemann

[1] The experimental values for chlorine are unpublished values measured by J. Eckerman of the U.S. Naval Ordnance Laboratory.

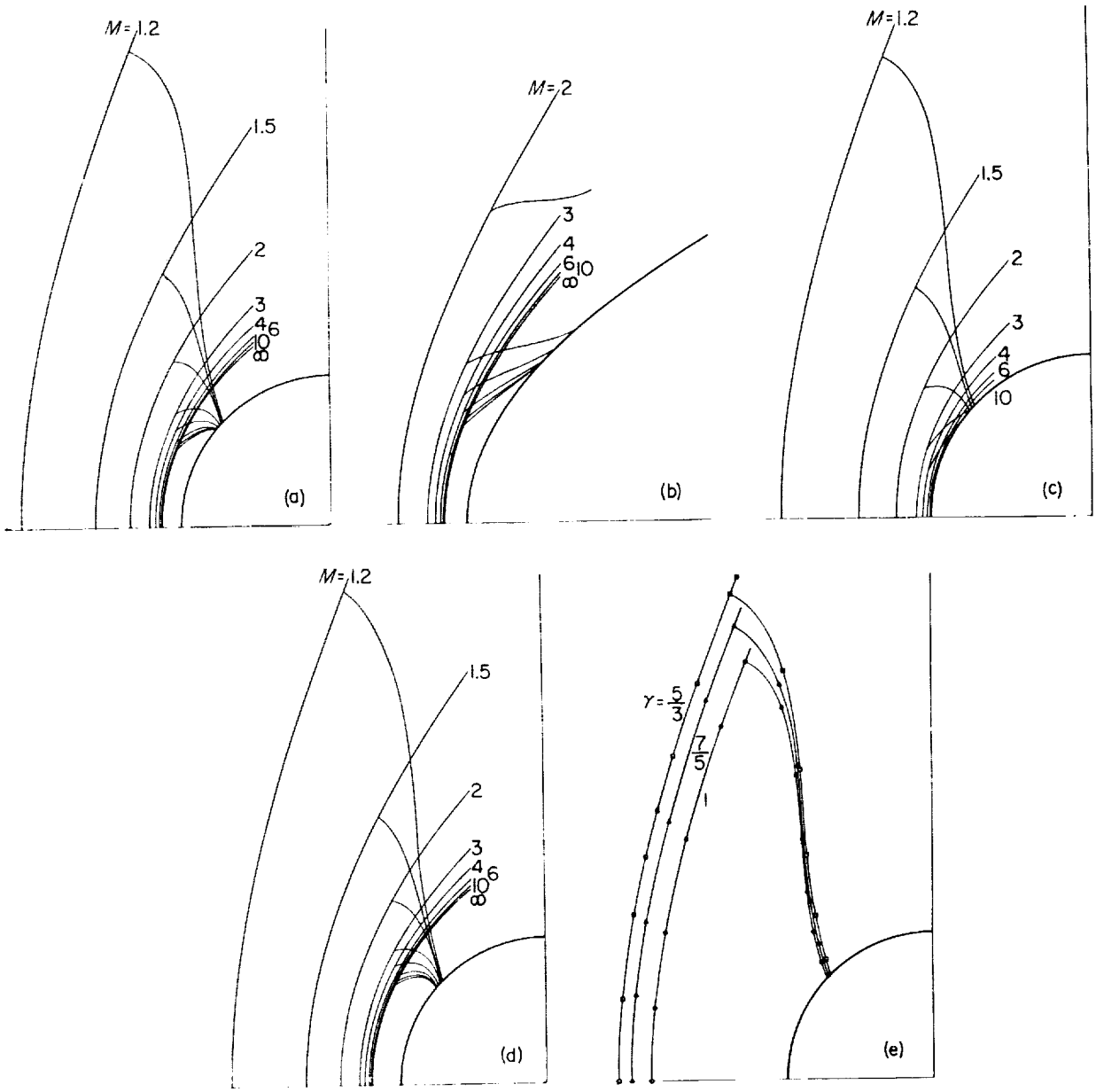

(a) Sphere with $\gamma=7/5$. (b) Paraboloid with $\gamma=7/5$. (c) Sphere with $\gamma=1$.
(d) Sphere with $\gamma=5/3$. (e) Sphere at $M=1.2$.

FIGURE 15.—Shape of shock wave and sonic line.

(see refs. 1 and 12 for discussion of that theory). For the sphere the surface pressure is given by

$$p_b=\frac{\sin 3\theta}{3\sin\theta}=1-\frac{4}{3}\sin^2\theta \qquad (21)$$

compared with the "simple Newtonian" value of $\cos^2\theta$. Figure 18(a) shows that the surface pressure distributions for $\gamma=1$ approach that limit as M increases, and linearly in $1/M^2$ as they should. Unfortunately, the present solutions do not extend to $\theta=60°$, where a zero in the surface pressure (cf. eq. (21)) and consequent singularities in higher approximations has led to some controversy regarding the proper interpretation of the Newtonian plus centrifugal theory. It would be necessary to extend the present solutions by the method of characteristics to resolve that difficulty.

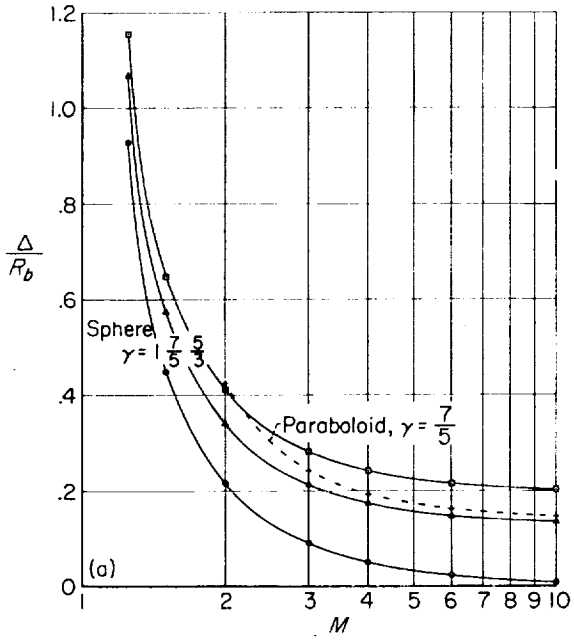

(a) Comparison of four cases.

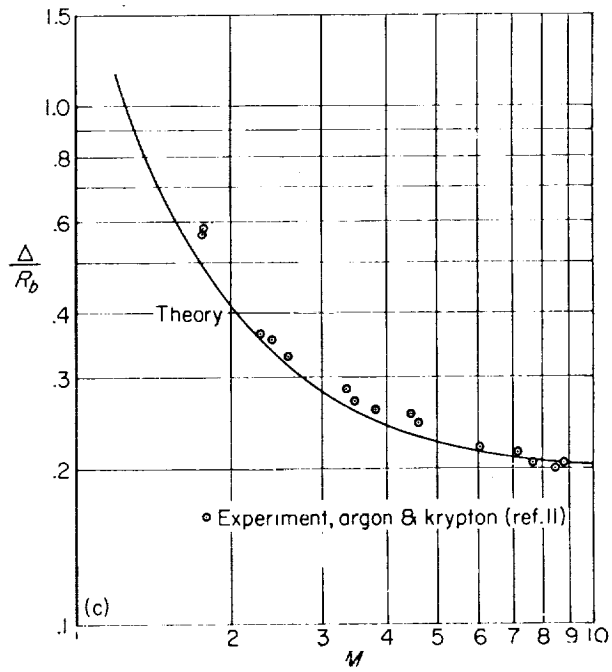

(c) Comparison with experiment for monatomic gas.

FIGURE 16.—Concluded.

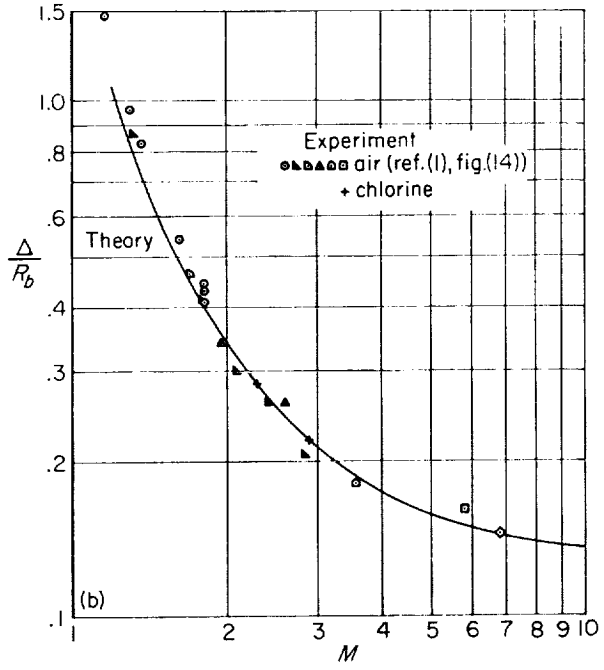

(b) Comparison with experiment for diatomic gas.

FIGURE 16.—Variation of stand-off distance with Mach number.

The effect of carrying out the Newtonian limiting process in reverse order, letting γ tend toward 1 at infinite Mach number, is shown in figure 18(b). The approach to the limit appears less "uniform" in this case. Each curve for $\gamma>1$ crosses the limiting one for $\gamma=1$, but the point of intersection moves rapidly. Its limit is given by Freeman's second approximation (ref. 13), which is otherwise, however, seen to be of little utility for γ appreciably different from 1.

Upstream limiting line.—One of the oldest analytical attacks on the blunt-body problem consists in expanding the flow field in Taylor series starting from the shock wave. It was suggested in reference 14 that this method will fail because the analytical continuation of the flow upstream through the shock wave contains a limiting line. If this limiting line is closer to the shock wave than is the body, the radius of convergence of Taylor series will not extend to the body. This conjecture has been investigated numerically for spheres with $\gamma=7/5$ for $M=1.5$, 3, and ∞. On the axis of symmetry the nose of the body is found to lie, respectively, at 3.2, 1.8, and 1.35 of the distance (in terms of η) to the limiting line. Hence the series cannot reach the body even at $M=\infty$.

Possible modifications and extensions of the numerical method.—Except for case 244, all final

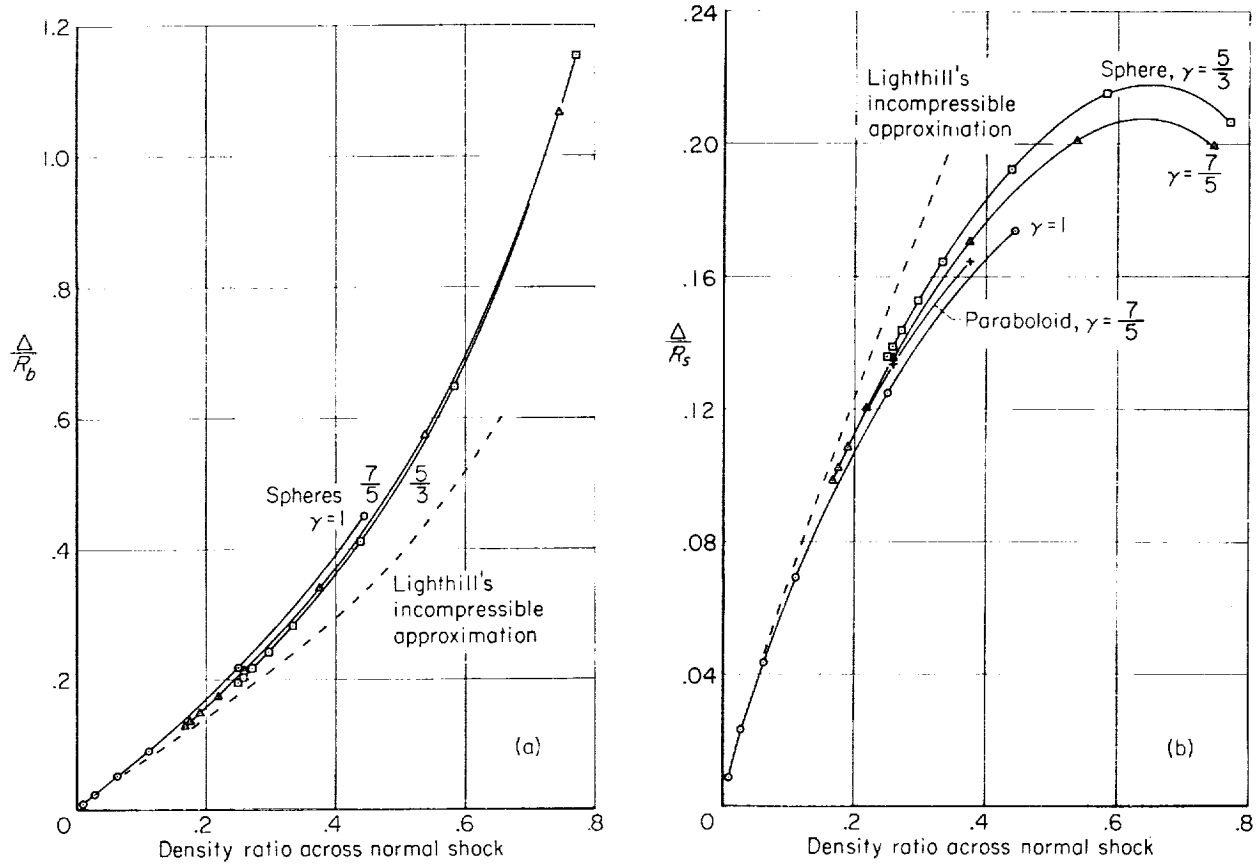

(a) Referred to radius for sphere.

(b) Referred to nose radius of shock wave.

FIGURE 17.—Correlation of stand-off distance according to density ratio across normal shock wave.

solutions were calculated without dropping end points, so that the outermost few points are affected by end instability. Repeating several cases shows that this difficulty can be entirely eliminated by dropping the 5 outermost points at each step and that the same range of body surface can be attained. Unfortunately, this procedure is not always applicable because so many points are dropped that one would have to include a portion of the shock wave beyond where it has degenerated to a Mach wave, which stops the solution. However, it has been noted that trial shows a 7-point differentiation scheme to be essentially as accurate as the 11-point one used. Hence it is suggested that future solutions should use a 7-point central difference scheme, dropping only 3 points at each step.

Two other modifications suggested previously should also be considered: elimination of division by zero in computing $\omega_{\eta\eta}$, and the use of "sheared Cartesian" coordinates (fig. 11).

The general idea of starting a numerical solution from an assumed shock wave is susceptible to many interesting variations. Currently noncircular cones in supersonic flow are being treated using the full inviscid equations by starting from an elliptical conical shock wave. Starting from a sinusoidal shock would probably lead to choked flow past a lattice. General three-dimensional problems could probably be handled with a larger computing machine; the initial attack might well start from elliptical-paraboloidal shock waves. Angle of attack could be considered by tilting the shock waves used here; the camber of the resulting body might be negligible back to the sonic line. This would be simpler in plane flow, where a stream function exists; but a pair of stream functions can be used for general three-dimensional flows.

AMES RESEARCH CENTER
NATIONAL AERONAUTICS AND SPACE ADMINISTRATION
MOFFETT FIELD, CALIF., *Oct. 2, 1958*

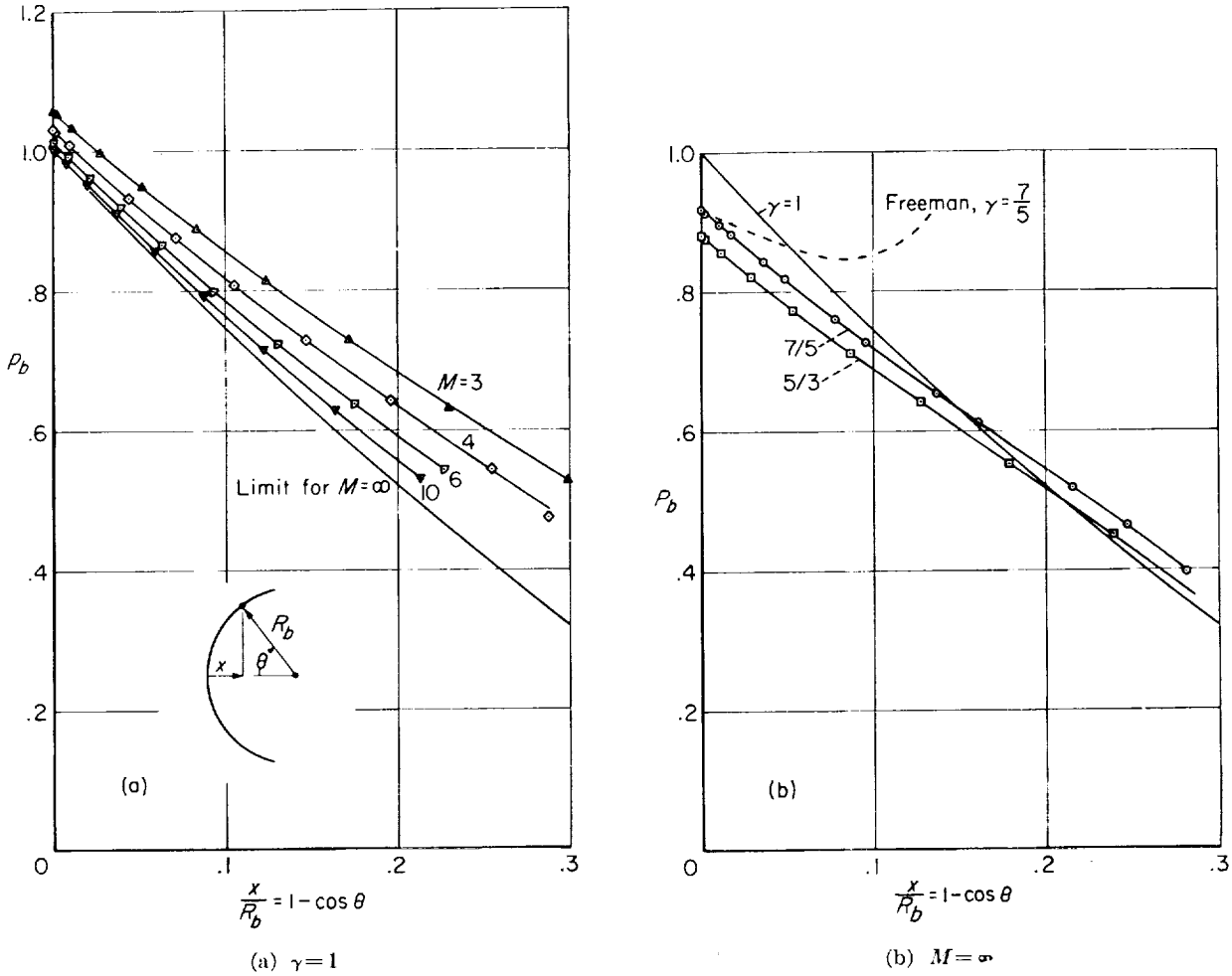

(a) $\gamma = 1$ (b) $M = \infty$

FIGURE 18.—Pressure distribution on sphere.

APPENDIX A

PRINCIPAL SYMBOLS

B	bluntness of conic section (see eq. (1))
C	$1-B_s$
D	denominator in computation of $\frac{\rho_\eta}{\rho}$
f	$\frac{p}{\rho^\gamma}$
M	free-stream Mach number
M_l	local Mach number
N	total number of points along shock wave
n	number of point along shock wave
p	pressure (referred to $\rho_\infty V_\infty^2$)
r	radius in cylindrical polar coordinates
R	nose radius
s	see equation (13c)
u, v	velocity components along ξ,η axes
V	velocity
x	abscissa
γ	adiabatic exponent
Δ	stand-off distance of shock wave from body
$\Delta\xi,\Delta\eta$	mesh widths
$\delta\eta$	see equation (16c)
η	curvilinear coordinate orthogonal to ξ
θ	local stream angle
ν	0 for plane, 1 for axisymmetric flow
ξ	curvilinear coordinate orthogonal to η
ρ	density (referred to ρ_∞)
ϕ	azimuthal angle
Ψ	stream function
ω	reduced stream function
$(\ )_s$	value associated with shock wave
$(\ )_b$	value associated with body
$(\ )_\infty$	free-stream value
$(\ )^{(m)}$	value at mth interval in ξ
${}^{(m)}(\ )$	value at mth interval in η
$(\ )_*$	value at sonic point on body
$(\ )_o$	value at vertex of body

REFERENCES

1. Van Dyke, Milton D.: The Supersonic Blunt-Body Problem—Review and Extension. Jour. Aero. Sci., vol. 25, no. 8, Aug. 1958, pp. 485–496.
2. Uchida, Shigeo, and Yasuhara, Michiru: The Rotational Field Behind a Curved Shock Wave Calculated by the Method of Flux Analysis. Jour. Aero. Sci., vol. 23, no. 9, Sept. 1956, pp. 830–845.
3. Mangler, K. W., and Evans, M. E.: The Calculation of the Inviscid Flow Between a Detached Bow Wave and a Body. R.A.E. Tech. Note Aero 2536, Oct. 1957.
4. Zlotnick, Martin, and Newman, Donald J.: Theoretical Calculation of the Flow on Blunt-Nosed Axisymmetric Bodies in a Hypersonic Stream. AVCO Mfg. Co., Rept. RAD-TR-2-57-29, Sept. 19, 1957.
5. Belotserkovsky, O. M.: Flow Past a Symmetrical Profile with a Detached Shock Wave. Prikl. Mat. i Mekh., vol. 22, no. 2, Mar.–Apr. 1958. pp. 206–219. (Russian)
6. Garabedian, P. R., and Lieberstein, H. M.: On the Numerical Calculation of Detached Bow Shock Waves in Hypersonic Flow. Jour. Aero. Sci., vol. 25, no. 2, Feb. 1958, pp. 109–118.
7. Ames Research Staff: Equations, Tables, and Charts for Compressible Flow. NACA Rep. 1135, 1953.
8. Bickley, W. G.: Formulae for Numerical Differentiation. Math. Gazette (London), vol. 25, 1941, pp. 19–27.
9. Drebinger, John W.: Detached Shock Waves. Ph. D. thesis, Harvard Univ., 1950.
10. Probstein, Ronald F.: On the Nature of the Sonic Line for Supersonic and Hypersonic Flow Over Blunt Bodies. Brown Univ., Div. of Eng., Sept. 1957.
11. Schwartz, R. N., and Eckerman, J.: Shock Location in Front of a Sphere as a Measure of Real Gas Effects. Jour. Appl. Phys., vol. 27, no. 2, Feb. 1956, pp. 169–174.
12. Lighthill, M. J.: Dynamics of a Dissociating Gas. Part I: Equilibrium Flow. Jour. Fluid Mech., vol. 2, pt. 1, Jan. 1957, pp. 1–32.
13. Freeman, N. C.: On the Theory of Hypersonic Flow Past Plane and Axially Symmetric Bluff Bodies. Jour. Fluid Mech., vol. 1, pt. 4, Oct. 1956, pp. 366–387.
14. Van Dyke, Milton D.: A Model of Supersonic Flow Past Blunt Axisymmetric Bodies, with Application to Chester's Solution. Jour. Fluid Mech., vol. 3. pt. 5, Feb. 1958, pp. 515–522.

TABLE I.—EPITOME OF MACHINE SOLUTION FOR SPHERE AT $M=\infty$, $\gamma=7/5$ (CASE 180)

η	ξ	ω	ω_ξ	ω_η	$\omega_{\eta\eta}$	ρ	ρ_η	p	M_l	D
1.00	0.0175	1.00000	0	12.000	37.441	6.0000	−9.7451	0.83104	0.39630	6.0000
	.0525	1.00000	0	12.000	39.403	6.0000	−8.6121	.82092	.46970	6.0000
	.0875	1.00000	0	12.000	42.945	6.0000	−6.5728	.80301	.58054	6.0000
	.1225	1.00000	0	12.000	48.086	6.0000	−3.6245	.77782	.71406	6.0000
	.1575	1.00000	0	12.000	54.866	6.0000	.2425	.74603	.86296	6.0000
	.1925	1.00000	0	12.000	63.356	6.0000	5.0515	.70844	1.0244	6.0000
	.2275	1.00000	0	12.000	73.676	6.0000	10.849	.66597	1.1980	6.0000
	.2625	1.00000	0	12.000	86.017	6.0000	17.715	.61954	1.3848	6.0000
	.2975	1.00000	0	12.000	100.67	6.0000	25.785	.57008	1.5867	6.0000
.98	.0175	.76749	.06430	11.251	43.372	6.1671	−6.9668	.86418	.31213	6.3871
	.0525	.76788	.06446	11.212	44.511	6.1450	−5.8894	.85179	.39115	6.3463
	.0875	.76859	.06529	11.141	46.535	6.1055	−3.9789	.82994	.50465	6.2725
	.1225	.76962	.06701	11.038	49.401	6.0491	−1.2816	.79934	.63670	6.1653
	.1575	.77097	.06975	10.903	53.051	5.9762	2.1416	.76095	.78080	6.0240
	.1925	.77267	.07454	10.733	57.415	5.8873	6.2213	.71590	.93488	5.8470
	.2275	.77474	.08216	10.526	62.417	5.7827	10.886	.66539	1.0989	5.6320
	.2625	.77720	.09408	10.280	67.978	5.6621	16.071	.61067	1.2739	5.3752
	.2975	.78013	.11204	9.9865	74.034	5.5249	21.726	.55288	1.4621	5.0711
.96	.0175	.55114	.23018	10.384	45.538	6.2843	−4.7540	.88779	.23700	6.4766
	.0525	.55254	.22937	10.322	45.951	6.2416	−3.7703	.87342	.32316	6.4006
	.0875	.55507	.23011	10.210	46.690	6.1658	−2.0459	.84812	.43912	6.2644
	.1225	.55873	.23265	10.050	47.745	6.0584	.3453	.81281	.56927	6.0694
	.1575	.56353	.23827	9.8417	49.106	5.9217	3.3074	.76871	.70881	5.8167
	.1925	.56950	.24939	9.5846	50.758	5.7577	6.7344	.71723	.85677	5.5076
	.2275	.57669	.26925	9.2781	52.700	5.5686	10.524	.65986	1.0138	5.1425
	.2625	.58521	.30225	8.9201	54.957	5.3555	14.598	.59805	1.1817	4.7209
	.2975	.59521	.35489	8.5059	57.628	5.1183	18.933	.53309	1.3631	4.2405
.94	.0175	.35257	.44717	9.4730	44.776	6.3610	−2.9165	.90349	.17010	6.3392
	.0525	.35530	.44367	9.4027	44.677	6.2998	−2.0451	.88745	.26552	6.2373
	.0875	.36020	.44222	9.2766	44.524	6.1915	−.5294	.85926	.38323	6.0561
	.1225	.36728	.44275	9.0954	44.356	6.0395	1.5474	.82001	.51074	5.7991
	.1575	.37652	.44751	8.8595	44.224	5.8478	4.0805	.77111	.64566	5.4705
	.1925	.38796	.46179	8.5694	44.189	5.6208	6.9600	.71419	.78835	5.0751
	.2275	.40167	.49173	8.2241	44.336	5.3624	10.094	.65093	.94036	4.6168
	.2625	.41779	.54652	7.8210	44.799	5.0751	13.442	.58285	1.1043	4.0981
	.2975	.43662	.64660	7.3533	45.868	4.7580	17.099	.51109	1.2844	3.5186
.92	.0175	.17207	.67525	8.5775	40.891	6.4036	−1.3372	.91241	.11424	6.0346
	.0525	.17618	.66857	8.5092	40.648	6.3260	−.5817	.89504	.22018	5.9170
	.0875	.18358	.66614	8.3861	40.206	6.1895	.7265	.86452	.33755	5.7088
	.1225	.19424	.66633	8.2082	39.562	5.9990	2.5066	.82205	.46100	5.4155
	.1575	.20817	.67235	7.9751	38.759	5.7604	4.6597	.76921	.59084	5.0439
	.1925	.22541	.69391	7.6856	37.915	.4803	7.0900	.70773	.72871	4.6012
	.2275	.24605	.73887	7.3374	37.164	5.1641	9.7339	.63935	.87715	4.0938
	.2625	.27034	.83158	6.9250	36.758	4.8144	12.628	.56545	1.0400	3.5250
	.2975	.29873	1.0158	6.4359	37.414	4.4263	16.071	.48656	1.2239	2.8920
.90	.0175	.00870	.89409	7.7597	−13.959	6.4161	.0813	.91533	.08288	5.6170
	.0525	.01413	.88253	7.6962	13.573	6.3246	.7287	.89693	.19153	5.4879
	.0875	.02389	.88030	7.5820	25.378	6.1638	1.8454	.86460	.30372	5.2688
	.1225	.03799	.88477	7.4170	29.845	5.9403	3.3583	.81960	.42071	4.9613
	.1575	.05642	.90305	7.1999	31.295	5.6620	5.1825	.76358	.54450	4.5739
	.1925	.07928	.93627	6.9273	31.348	5.3370	7.2406	.69830	.67761	4.1150
	.2275	.10674	1.0099	6.5941	30.631	4.9716	9.5158	.62539	.82357	3.5913
	.2625	.13919	1.1813	6.1898	30.243	4.5665	12.158	.54580	.98802	3.0043
	.2975	.17749	1.5200	5.6876	30.840	4.1071	15.850	.45859	1.1820	2.3433
.88	.0175	−.14929	1.1785	8.0388	2.4130	6.3981	1.7254	.91212	.10167	5.1082
	.0525	−.13708	.42060	7.4248	34.572	6.2961	2.1166	.89331	.18531	4.9869
	.0875	−.12267	.81210	7.0745	42.736	6.1152	3.0129	.85973	.28411	4.7700
	.1225	−.10438	1.0115	6.8201	47.376	5.8640	4.2700	.81284	.39119	4.4659
	.1575	−.08132	1.0804	6.5740	67.507	5.5523	5.7843	.75435	.50735	4.0837
	.1925	−.05300	1.1143	6.3004	10.123	5.1896	7.4965	.68600	.63529	3.6320
	.2275	−.01902	1.3265	5.9815	22.552	4.7813	9.5140	.60900	.77969	3.1162
	.2625	.02144	1.5795	5.5850	24.798	4.3248	12.017	.52362	.94846	2.5329
	.2975	.06991	2.4793	5.0708	26.036	3.7797	16.883	.42507	1.1625	1.8551

TABLE I.—EPITOME OF MACHINE SOLUTION FOR SPHERE AT $M=\infty$, $\gamma=7/5$ (CASE 180)—Concluded

η	ξ	ω	ω_ξ	ω_η	$\omega_{\eta\eta}$	ρ	ρ_η	p	M_t	D
. 86	. 0175	−. 30958	. 16746	7. 9906	8. 2739	6. 3431	3. 7664	. 90158	. 15945	4. 5343
	. 0525	−. 27866	−1. 4840	6. 7333	40. 568	6. 2411	3. 3883	. 88427	. 20331	4. 4367
	. 0875	−. 25561	. 26120	6. 2197	45. 834	6. 0458	3. 9338	. 85026	. 28091	4. 2345
	. 1225	−. 23131	. 25014	5. 8726	33. 012	5. 7732	4. 8147	. 80225	. 37438	3. 9454
	. 1575	−. 19929	−43. 204	5. 2238	−203. 43	5. 5062	−1. 1779	. 75539	. 45453	3. 5470
	. 1925	−. 17698	−25. 505	6. 0979	−1531. 8	5. 1169	−. 2274	. 68623	. 57105	3. 1645
	. 2275	−. 13414	1. 2243	5. 5305	−183. 72	4. 5888	9. 7366	. 58992	. 74579	2. 6697
	. 2625	−. 08530	1. 9127	5. 0890	5. 4146	4. 0818	12. 278	. 49831	. 92243	2. 1054
	. 2975	−. 02630	4. 7759	4. 5501	26. 470	3. 4037	20. 723	. 38056	1. 1784	1. 4049

TABLE II.—SUMMARY OF PRELIMINARY SOLUTIONS

Case No.	M	γ	B_s	$\Delta\xi$	$\Delta\eta$	N	$\frac{\Delta}{R_s}$	$\frac{R_b}{R_s}$	$\frac{\Delta}{R_b}$	B_b	Steps to nose
17	2. 408	1. 4	−0. 03064	0. 05	0. 05	20	0. 1515	0. 57	0. 266	0. 97	4
24	5. 8	1. 4	. 14	. 04	. 04	20	. 1081	. 710	. 152	. 70	3
27	10^4	1. 4	0	. 025	. 015	20	. 0982	. 726	. 135	. 35	7
29	2	1. 4	0	. 025	. 04	20	. 1705	. 508	. 336	1. 16	5
35	5. 8	1. 4	. 25	. 05	. 04	20	. 1080	. 710	. 152	. 85	3
36	5. 8	1. 4	. 30	. 05	. 04	20	. 1083	. 727	. 149	. 99	3
40	10^4	1. 2	0	. 05	. 02	20	. 05942	. 817	. 073	. 29	3
41	10^4	1. 1	0	. 05	. 01	20	. 03436	. 888	. 0387	. 20	4
42	10^4	1. 05	0	. 05	. 005	20	. 01919	. 934	. 0205	. 10	4
43	10^4	1. 025	0	. 05	. 0025	20	. 01032	. 964	. 0107	. 07	5
44	10^4	1. 4	1. 25	. 03	. 03	20	. 09827	. 836	. 118	2. 33	4
45	10^4	1. 4	1. 00	. 035	. 03	20	. 09808	. 810	. 121	1. 85	4
46	10^4	1. 4	. 75	. 04	. 03	20	. 0979	. 780	. 126	1. 40	4
48	10^4	1. 4	. 25	. 045	. 03	20	. 0975	. 74	. 132	. 65	4
49	10^4	1. 4	0	. 05	. 03	20	. 0973	. 720	. 135	. 33	4
50	10^4	1. 4	−. 25	. 055	. 03	20	. 0973	. 706	. 138	. 04	4
51	10^4	1. 4	−. 50	. 06	. 03	20	. 0972	. 685	. 142	−. 25	4
52	1. 3	1. 4	−2. 6	. 035	. 06	20	. 2005	. 22	. 91	. 8	5
53	1. 81	1. 4	−. 8	. 035	. 06	20	. 1778	. 404	. 440	. 52	4
54	2. 81	1. 4	0	. 04	. 05	20	. 1384	. 595	. 233	. 70	3
55	3. 52	1. 4	. 1	. 05	. 05	20	. 1245	. 645	. 360	. 72	3
56	14. 2	1. 3	−. 5	. 04	. 03	20	. 0819	. 725	. 113	−. 26	3
57	14. 2	1. 35	−. 5	. 04	. 03	20	. 0908	. 698	. 130	−. 13	4
59	10^4	1. 4	. 5	. 04	. 03	20	. 0977	. 763	. 128	1. 0	4
60	10^4	5/3	0	. 05	. 06	20	. 13386	. 646	. 207	. 43	3
64	14. 2	1. 3	. 5	. 04	. 03	20	. 0819	. 791	. 104	1. 12	3
65	14. 2	1. 35	. 5	. 04	. 03	20	. 0910	. 770	. 118	1. 0	4
66	2	1. 4	−. 27	. 035	. 06	20	. 1686	. 4814	. 350	. 82	4
67	20	1. 4	0	. 025	. 025	20	. 0987	. 721	. 137	. 38	5
69	12	1. 4	−. 006993	. 05	. 03	20	. 1000	. 714	. 140	. 34	4
70	2	1. 4	−. 2	. 035	. 06	20	. 16918	. 490	. 345	. 88	4
71	20	1. 4	0	. 05	. 025	20	. 0987	. 720	. 137	. 32	5
86	2	1. 4	−1. 5	. 03	. 04	20	. 16444	. 38	. 43	0	6
87	2	1. 4	−1. 0	. 03	. 04	20	. 16628	. 413	. 403	. 22	6
88	2	1. 4	−. 5	. 03	. 04	20	. 16827	. 458	. 367	. 59	5
89	2	1. 4	0	. 03	. 04	20	. 17048	. 506	. 337	1. 06	5
91	3	1. 4	−1. 00	. 04	. 03	20	. 13275	. 513	. 259	. 33	6
92	3	1. 4	−. 75	. 04	. 03	20	. 13220	. 535	. 247	−. 15	6
93	3	1. 4	−. 50	. 04	. 03	20	. 13344	. 554	. 241	. 06	5
94	3	1. 4	−. 25	. 04	. 03	20	. 13412	. 584	. 230	. 38	5

TABLE II.- SUMMARY OF PRELIMINARY SOLUTIONS—Concluded

Case No.	M	γ	B_s	$\Delta\xi$	$\Delta\eta$	N	$\frac{\Delta}{R_s}$	$\frac{R_b}{R_s}$	$\frac{\Delta}{R_b}$	B_b	Steps to nose
95	3	1.4	0	0.01	.03	20	0.13466	0.609	0.221	0.67	5
96	3	1.4	.25	.01	.03	20	.13524	.637	.212	1.02	5
97	3	1.4	.50	.04	.03	20	.13561	.657	.206	1.25	5
99	4	1.4	−1.00	.05	.025	20	.11841	.546	.217	−.61	6
100	4	1.4	−.50	.04	.025	20	.11897	.606	.196	−.08	6
101	4	1.4	0	.04	.025	20	.11958	.647	.185	.50	6
102	4	1.4	.50	.04	.025	20	.12026	.701	.172	1.16	5
103	4	1.4	1.00	.03	.025	20	.12103	.752	.161	1.91	5
104	6	1.4	−.75	.07	.02	20	.10740	.622	.173	−.48	6
106	6	1.4	−.25	.05	.02	20	.10780	.666	.162	.05	6
108	6	1.4	.25	.035	.02	20	.10825	.713	.152	.69	6
110	6	1.4	.75	.03	.02	20	.10874	.759	.143	1.41	6
112	6	1.4	1.25	.025	.02	20	.10930	.810	.135	2.31	6
113	10	1.4	−.5	.06	.02	20	.10133	.668	.152	−.29	6
114	10	1.4	0	.04	.02	20	.10165	.712	.143	.34	6
115	10	1.4	.5	.03	.02	20	.10201	.756	.135	1.02	6
116	10	1.4	1.0	.03	.02	20	.10243	.804	.127	1.86	6
117	10	1.4	1.5	.025	.02	20	.10289	.848	.121	2.69	5
121	2	1	.4	.03	.04	20	.12496	.602	.208	1.36	4
122	10^4	5/3	.25	.04	.03	20	.13539	.669	.202	.67	5
123	1.5	1.4	−1.0	.02	.05	20	.19881	.331	.601	.84	5
124	1.5	1.4	−.5	.02	.05	20	.20262	.367	.552	1.16	5
125	1.5	1.4	0	.02	.05	20	.20719	.414	.500	1.48	5
129	2	1	0	.025	.025	20	.12489	.575	.217	.99	6
130	4	1	.6	.035	.015	20	.04303	.855	.0503	1.12	3
131	4	1	.8	.035	.015	20	.04300	.865	.0497	1.44	3
132	10^4	5/3	.5	.04	.025	20	.13612	.700	.194	1.06	6
133	4	5/3	.25	.04	.025	20	.15276	.620	.246	.88	7
134	4	5/3	.4	.04	.025	20	.15323	.637	.241	1.06	7
135	2	5/3	0	.03	.04	20	.19266	.475	.406	1.07	6
136	2	5/3	−.25	.03	.04	20	.19100	.448	.426	.83	6
137	2	5/3	−.50	.03	.04	20	.18934	.422	.449	.60	6
139	1.2	1.4	−1	.02	.06	11	.22021	.287	.767	1.7	5
149	10^4	1.4	.5	.035	.02	20	.09830	.767	.128	1.00	6
151	10^4	15/13	0	.05	.01	20	.04891	.849	.0576	.20	6
160	1.2	1.4	−3	.025	.06	20	.20163	.196	1.029	1.08	6
165	10^4	1.4	.25	.04	.02	20	.09812	.746	.132	.65	6
166	10^4	1.4	−.25	.04	.02	20	.09782	.705	.139	0	6
187	1.2	1	−3	.025	.05	16	.18842	.213	.885	1.19	6
188	1.5	1	−.6	.025	.038	18	.17382	.393	.442	1.05	6

TABLE III.—SUMMARY OF FINAL SOLUTIONS FOR SPHERES AND PARABOLOIDS

Case no.	Body shape	M	γ	B_s	$\Delta\xi$	$\Delta\eta$	N	$\frac{\Delta}{R_s}$	$\frac{R_b}{R_s}$	$\frac{\Delta}{R_b}$	Steps to nose
173	Sphere	1.2	1.4	−3.30	0.025	0.06	16	0.19227	0.187	1.066	6
174	↓	1.5	1.4	−.71	.025	.045	18	.20094	.350	.574	6
175		2	1.4	−.06	.03	.04	20	.17020	.500	.340	5
176		3	1.4	.25	.035	.03	20	.13505	.634	.213	5
177		4	1.4	.38	.035	.025	20	.12009	.6895	.174	6
178		6	1.4	.47	.03	.02	20	.10845	.732	.148	6
179		10	1.4	.49	.032	.02	20	.10201	.7535	.135	6
180		10^4	1.4	.50	.035	.02	20	.09828	.7662	.128	6
181	Paraboloid	2	1.4	−1.50	.04	.04	20	.16442	.387	.425	6
182	↓	3	1.4	−.59	.05	.03	20	.13344	.550	.243	6
183		4	1.4	−.41	.055	.025	20	.11908	.613	.194	6
184		6	1.4	−.30	.06	.02	20	.10776	.662	.163	6
185		10	1.4	−.26	.06	.02	20	.10148	.689	.147	6
186		10^4	1.4	−.25	.06	.02	20	.09782	.705	.139	6
244	Sphere	1.2	1	−3.28	.025	.05	[a]45	.18648	.201	.928	6
240	↓	1.5	1	−.69	.025	.038	18	.17337	.386	.449	6
189		2	1	.01	.032	.025	20	.12488	.573	.218	6
223		3	1	.35	.035	.014	20	.06908	.764	.0904	6
224		4	1	.51	.035	.008	20	.04338	.854	.0508	6
225		6	1	.67	.035	.0045	20	.02156	.931	.0232	5
226		10	1	.80	.035	.0018	20	.00855	.976	.00816	5
194	Sphere	1.2	5/3	−3.32	.025	.07	16	.20651	.179	1.154	5
195	↓	1.5	5/3	−.73	.025	.055	18	.21500	.332	.648	5
196		2	5/3	−.08	.03	.04	20	.19213	.467	.411	6
197		3	5/3	.22	.035	.036	20	.16446	.584	.282	5
198		4	5/3	.35	.035	.032	20	.15284	.631	.242	6
199		6	5/3	.43	.030	.03	20	.14373	.666	.216	6
200		10	5/3	.46	.032	.03	20	.13875	.684	.203	5
201		10^4	5/3	.47	.035	.03	20	.13585	.695	.195	5

[a] 5 points dropped each step.

TABLE IV.—GEOMETRY AND PRESSURE DATA FOR SPHERES AND PARABOLOIDS

Case 173: Sphere at $M=1.2$, $\gamma=7/5$

Shock		Sonic line [a]		Body			
x/R_s	r/R_s	x/R_s	r/R_s	n	x/R_s	r/R_s	p_b
0	0	0.1411	0.5898	0	0.1993	0	[b]1.186
.006	.1101	.1994	.5139	2	.2011	.0257	1.168
.02	.2033	.2161	.4001	4	.2089	.0593	1.096
.05	.3290	.2221	.3004	6	.2232	.0915	.966
.10	.4827	.2305	.2272	8	.2440	.1213	.768
.15	.6118	.2411	.1732	10	.2736	.1460	-------
.20	.7294	.2529	.1326				

[a] First 5 values from supplementary case 241.
[b] Exact: 1.1942.

Case 174: Sphere at $M=1.5$, $\gamma=7/5$

Shock		Sonic line [a]		Body			
x/R_s	r/R_s	x/R_s	r/R_s	n	x/R_s	r/R_s	p_b
0	0	0.1627	0.5867	0	0.2009	0	[b]1.081
.02	.2007	.2014	.5430	2	.2020	.0283	1.075
.05	.3190	.2270	.4850	4	.2071	.0658	1.050
.10	.4551	.2460	.4240	6	.2163	.1028	1.004
.15	.5621	.2617	.3652	8	.2296	.1390	.941
.20	.6545	.2763	.3116	10	.2471	.1741	.859
.30	.8148	.2907	.2640	12	.2688	.2077	.744
.40	.9558			14	.2954	.2390	.587
				16	.3335	.2632	-------

[a] First 5 values from supplementary case 242. Last 2 from supplementary case 233.
[b] Exact: 1.0836.

TABLE IV.—GEOMETRY AND PRESSURE DATA FOR SPHERES AND PARABOLOIDS—Continued

Case 175: Sphere at $M=2$, $\gamma=7/5$

Shock	
x/R_s	r/R_s
0	0
.05	.3165
.1	.4479
.2	.6344
.3	.7781
.4	.8998
.5	1.0075

[a] Exact: 1.0072.

Sonic line	
x/R_s	r/R_s
0.1496	0.5482
.1949	.5365
.2298	.5092
.2568	.4722
.2780	.4297
.2950	.3838

Body			
n	x/R_s	r/R_s	p_b
0	0.1702	0	[a]1.007
2	.1716	.0365	1.002
4	.1775	.0849	.980
6	.1881	.1330	.942
8	.2039	.1802	.888
10	.2245	.2264	.817
12	.2501	.2712	.731
14	.2810	.3140	.631
16	.3180	.3540	.499
18	.3644	.3880	.247

Case 176: Sphere at $M=3$, $\gamma=7/5$

Shock	
x/R_s	r/R_s
0	0
.02	.1998
.05	.3152
.1	.4444
.2	.6245
.3	.7600
.4	.8718

[a] Exact: 0.9572.

Sonic line	
x/R_s	r/R_s
0.1161	0.4784
.1599	.4928
.1982	.4958
.2314	.4900
.2595	.4764
.2826	.4559
.3008	.4291
.3160	.3990

Body			
n	x/R_s	r/R_s	p_b
0	0.1350	0	[a]0.957
2	.1367	.0450	.952
4	.1438	.1048	.929
6	.1568	.1641	.890
8	.1757	.2228	.834
10	.2006	.2805	.766
12	.2317	.3367	.685
14	.2696	.3910	.590
16	.3150	.4422	.469
18	.3710	.4874	.270

Case 177: Sphere at $M=4$, $\gamma=7/5$

Shock	
x/R_s	r/R_s
0	0
.02	.1996
.05	.3147
.1	.4429
.2	.6203
.3	.7522
.4	.8598

[a] Exact: 0.9405.

Sonic line	
x/R_s	r/R_s
0.1002	0.4433
.1398	.4646
.1764	.4777
.2097	.4836
.2393	.4826
.2648	.4751
.2859	.4611
.3024	.4408

Body			
n	x/R_s	r/R_s	p_b
0	0.1201	0	[a]0.940
2	.1216	.0459	.935
4	.1285	.1070	.915
6	.1409	.1678	.878
8	.1590	.2280	.828
10	.1829	.2874	.776
12	.2128	.3456	.689
14	.2494	.4023	.601
16	.2931	.4565	.494
17	.3182	.4822	.429

Case 178: Sphere at $M=6$, $\gamma=7/5$

Shock	
x/R_s	r/R_s
0	0
.02	.1995
.05	.3144
.1	.4419
.2	.6174
.3	.7468
.4	.8514

[a] Exact: 0.9289.

Sonic line	
x/R_s	r/R_s
0.0880	0.4153
.1218	.4391
.1544	.4579
.1853	.4717
.2141	.4805
.2402	.4838
.2628	.4814
.2783	.4679

Body			
n	x/R_s	r/R_s	p_b
0	0.1084	0	[a]0.928
2	.1096	.0400	.925
4	.1144	.0932	.911
6	.1232	.1462	.886
8	.1361	.1990	.850
10	.1530	.2513	.804
12	.1742	.3032	.750
14	.1998	.3543	.687
16	.2301	.4043	.616
18	.2654	.4531	.530
19	.2850	.4769	.466

Case 179: Sphere at $M=10$, $\gamma=7/5$

Shock	
x/R_s	r/R_s
0	0
.02	.1995
.05	.3143
.1	.4417
.2	.6168
.3	.7456
.4	.8495

[a] Exact: 0.9230.

Sonic line	
x/R_s	r/R_s
0.0820	0.4008
.1168	.4284
.1511	.4513
.1841	.4695
.2151	.4821
.2431	.4886
.2679	.4893
.2871	.4814

Body			
n	x/R_s	r/R_s	p_b
0	0.1020	0	[a]0.923
2	.1032	.0430	.919
4	.1087	.1002	.903
6	.1186	.1572	.876
8	.1331	.2139	.836
10	.1521	.2702	.786
12	.1760	.3259	.727
14	.2051	.3807	.658
16	.2396	.4344	.580
18	.2803	.4861	.490
19	.3038	.5107	.427

Case 180: Sphere at $M=\infty$, $\gamma=7/5$

Shock	
x/R_s	r/R_s
0	0
.02	.1995
.05	.3142
.1	.4416
.2	.6164
.3	.7450
.4	.8485

[a] Exact: 0.9197.

Sonic line	
x/R_s	r/R_s
0.0784	0.3921
.1140	.4221
.1493	.4478
.1836	.4686
.2160	.4837
.2455	.4924
.2706	.4934
.2914	.4879

Body			
n	x/R_s	r/R_s	p_b
0	0.0983	0	[a]0.920
2	.0997	.0472	.915
4	.1063	.1100	.897
6	.1180	.1726	.864
8	.1352	.2349	.818
10	.1580	.2966	.760
12	.1867	.3575	.691
14	.2217	.4173	.612
16	.2636	.4753	.519
18	.3140	.5302	.398

TABLE IV.—GEOMETRY AND PRESSURE DATA FOR SPHERES AND PARABOLOIDS—Continued

Case 181: Paraboloid at $M=2$, $\gamma=7/5$

Shock	
x/R_s	r/R_s
0	0
.02	.2015
.05	.3221
.1	.4637
.2	.6782
.3	.8573
.4	1.0198

[a]Exact: 1.0072.

Sonic line	
x/R_s	r/R_s
0.2266	0.7281
.3112	.7538
.3841	.7583
.4716	.7799

Body			
n	x/R_s	r/R_s	p_b
0	0.1644	0	[a]1.004
2	.1673	.0476	.994
4	.1801	.1104	.951
6	.2027	.1718	.887
8	.2343	.2312	.817
10	.2736	.2885	.754
12	.3196	.3439	.706
14	.3711	.3979	.670
16	.4270	.4508	.645
17	.4563	.4772	.635

Case 182: Paraboloid at $M=3$, $\gamma=7/5$

Shock	
x/R_s	r/R_s
0	0
.02	.2006
.05	.3186
.1	.4538
.2	.6508
.3	.8082
.4	.9457
.5	1.0712

[a]Exact: 0.9559.

Sonic line	
x/R_s	r/R_s
0.1363	0.5326
.1885	.5550
.2379	.5698
.2858	.5804
.3342	.5896
.3853	.6004
.4429	.6162
.5198	.6485

Body			
n	x/R_s	r/R_s	p_b
0	0.1334	0	[a]0.956
2	.1371	.0637	.945
4	.1531	.1480	.899
6	.1816	.2311	.830
8	.2218	.3123	.751
10	.2728	.3913	.675
12	.3335	.4684	.609
14	.4027	.5437	.556
16	.4793	.6178	.515
18	.5622	.6914	.481

Case 183: Paraboloid at $M=4$, $\gamma=7/5$

Shock	
x/R_s	r/R_s
0	0
.02	.2004
.05	.3178
.1	.4518
.2	.6453
.3	.7981
.4	.9304

[a]Exact: 0.9405.

Sonic line	
x/R_s	r/R_s
0.1082	0.4704
.1588	.5095
.2033	.5316
.2474	.5508
.2930	.5692
.3418	.5892
.3965	.6133
.4628	.6462

Body			
n	x/R_s	r/R_s	p_b
0	0.1191	0	[a]0.940
2	.1232	.0717	.928
4	.1415	.1667	.879
6	.1740	.2604	.804
8	.2200	.3522	.720
10	.2785	.4421	.638
12	.3485	.5300	.568
14	.4286	.6163	.511
16	.5179	.7015	.467
18	.6152	.7862	.428

Case 184: Paraboloid at $M=6$, $\gamma=7/5$

Shock	
x/R_s	r/R_s
0	0
.02	.2003
.05	.3174
.1	.4506
.2	.6419
.3	.7918
.4	.9209

[a]Exact: 0.9405.

Sonic line	
x/R_s	r/R_s
0.0981	0.4461
.1360	.4753
.1731	.4993
.2118	.5232
.2523	.5471
.2955	.5721
.3435	.6003
.3997	.6345
.4713	.6808

Body			
n	x/R_s	r/R_s	p_b
0	0.1078	0	[a]0.928
2	.1125	.0795	.915
4	.1334	.1849	.861
6	.1705	.2890	.779
8	.2232	.3913	.689
10	.2903	.4916	.603
12	.3708	.5902	.530
14	.4634	.6873	.471
16	.5668	.7837	.426

Case 185: Paraboloid at $M=10$, $\gamma=7/5$

Shock	
x/R_s	r/R_s
0	0
.02	.2003
.05	.3172
.1	.4501
.2	.6406
.3	.7896
.4	.9174

[a]Exact: 0.9230.

Sonic line	
x/R_s	r/R_s
0.0903	0.4274
.1285	.4591
.1677	.4887
.2090	.5182
.2534	.5487
.3027	.5823
.3602	.6218
.4327	.6729
.5379	.7494

Body			
n	x/R_s	r/R_s	p_b
0	0.1015	0	[a]0.923
2	.1061	.0802	.910
4	.1266	.1866	.857
6	.1631	.2918	.777
8	.2150	.3955	.688
10	.2813	.4975	.603
12	.3610	.5980	.530
14	.4531	.6972	.470
16	.5564	.7957	.422

Case 186: Paraboloid at $M=\infty$, $\gamma=7/5$

Shock	
x/R_s	r/R_s
0	0
.02	.2002
.05	.3172
.1	.4500
.2	.6403
.3	.7890
.4	.9165

[a]Exact: 0.9194.

Sonic line	
x/R_s	r/R_s
0.0860	0.4170
.1248	.4510
.1653	.4838
.2085	.5171
.2560	.5527
.3105	.5932
.3770	.6429
.4674	.7115
.6024	.8112

Body			
n	x/R_s	r/R_s	p_b
0	0.0978	0	[a]0.920
2	.1024	.0806	.907
4	.1227	.1875	.855
6	.1589	.2934	.776
8	.2103	.3979	.688
10	.2760	.5009	.604
12	.3553	.6024	.531
14	.4468	.7029	.472
16	.5496	.8028	.424
17	.6048	.8529	.404

TABLE IV.—GEOMETRY AND PRESSURE DATA FOR SPHERES AND PARABOLOIDS—Continued

Case 244: Sphere at $M=1.2$, $\gamma=1$

Shock	
x/R_s	r/R_s
0	0
.005	.1004
.02	.2032
.05	.3289
.10	.4825
.15	.6114
.20	.7288
.25	.8396

Sonic line	
x/R_s	r/R_s
0.1339	0.5715
.1828	.5082
.2016	.4158
.2090	.3277
.2158	.2566
.2246	.2024
.2347	.1603

Body			
n	x/R_s	r/R_s	p_b
0	0.1865	0	[a]1.419
2	.1882	.0268	1.404
4	.1962	.0620	1.335
6	.2105	.0957	1.191
8	.2315	.1270	.992
10	.2614	.1534	.836
11	.2881	.1584	.582

[a] Exact: 1.4150.

Case 223: Sphere at $M=3$, $\gamma=1$

Shock	
x/R_s	r/R_s
0	0
.02	.1996
.05	.3148
.1	.4433
.2	.6213
.3	.7540
.4	.8626

Sonic line	
x/R_s	r/R_s
0.0524	0.3222
.0773	.3499
.1090	.3910
.1357	.4155
.1630	.4388
.1906	.4603
.2178	.4790
.2459	.4974

Body			
n	x/R_s	r/R_s	p_b
0	0.0691	0	[a]1.0572
2	.0707	.0488	1.0545
4	.0776	.1137	1.0330
6	.0903	.1783	.9981
8	.1086	.2423	.9491
10	.1329	.3056	.8873
12	.1634	.3678	.8143
14	.2004	.4285	.7295
16	.2447	.4870	.6308
18	.2976	.5418	.5027

[a] Exact: 1.05713.

Case 240: Sphere at $M=1.5$, $\gamma=1$

Shock	
x/R_s	r/R_s
0	0
.005	.2593
.02	.5199
.05	.8263
.1	1.1784
.15	1.4552
.20	1.6941
.25	1.9092
.30	2.1080

Sonic line [a]	
x/R_s	r/R_s
0.1420	0.5458
.1771	.5149
.2026	.4720
.2222	.4244
.2513	.3276
.2651	.2852

Body			
n	x/R_s	r/R_s	p_b
0	0.1734	0	[b]1.247
2	.1744	.0298	1.241
4	.1795	.0694	1.218
6	.1888	.1084	1.177
8	.2021	.1467	1.118
10	.2197	.1839	1.042
12	.2416	.2195	.937
14	.2684	.2530	.800
16	.3020	.2826	.614

[a] First 4 values from supplementary case 245.
[b] Exact: 1.2488.

Case 224: Sphere at $M=1$, $\gamma=1$

Shock	
x/R_s	r/R_s
0	0
.02	.1995
.05	.3142
.1	.4415
.2	.6161
.3	.7444
.4	.8476

Sonic line	
x/R_s	r/R_s
0.0301	0.2445
.0456	.2715
.0631	.3017
.0831	.3353
.1058	.3719
.1313	.4103
.1591	.4487
.1875	.4839
.2156	.5150

Body			
n	x/R_s	r/R_s	p_b
0	0.0434	0	[a]1.0319
2	.0449	.0502	1.0277
4	.0515	.1170	1.0097
6	.0635	.1837	.9776
8	.0810	.2500	.9324
10	.1041	.3159	.8756
12	.1332	.3810	.8075
14	.1686	.4452	.7294
16	.2108	.5080	.6411
18	.2608	.5686	.5445
19	.2892	.5976	.4740

[a] Exact: 1.03174.

Case 189: Sphere at $M=2$, $\gamma=1$

Shock	
x/R_s	r/R_s
0	0
.02	.2000
.05	.3162
.1	.4471
.2	.6321
.3	.7740
.4	.8935

Sonic line	
x/R_s	r/R_s
0.1054	0.4589
.1380	.4640
.1666	.4613
.1920	.4529
.2143	.4397
.2337	.4224
.2504	.4017
.2650	.3786

Body			
n	x/R_s	r/R_s	p_b
0	0.1249	0	[a]1.132
2	.1264	.0416	1.127
4	.1331	.0968	1.105
6	.1453	.1515	1.065
8	.1629	.2053	1.010
10	.1862	.2580	.938
12	.2153	.3090	.852
14	.2508	.3576	.743
16	.2941	.4023	.571
17	.3212	.4212	.359

[a] Exact: 1.1332.

Case 225: Sphere at $M=6$, $\gamma=1$

Shock	
x/R_s	r/R_s
0	0
.02	.1993
.05	.3136
.1	.4397
.2	.6109
.3	.7346
.4	.8324

Sonic line	
x/R_s	r/R_s
0.0136	0.1644
.0233	.1928
.0358	.2293
.0531	.2770
.0775	.3375
.1093	.4046
.1458	.4690
.1833	.5253

Body			
n	x/R_s	r/R_s	p_b
0	0.0216	0	[a]1.0139
2	.0230	.0514	1.0100
4	.0294	.1198	.9930
6	.0409	.1881	.9630
8	.0578	.2563	.9200
10	.0801	.3242	.8651
12	.1083	.3918	.7994
14	.1426	.4589	.7232
16	.1838	.5251	.6375
18	.2325	.5902	.5434

[a] Exact: 1.01398.

TABLE IV.—GEOMETRY AND PRESSURE DATA FOR SPHERES AND PARABOLOIDS—Continued

Case 226: Sphere at $M=10$, $\gamma=1$

Shock	
x/R_s	r/R_s
0	0
.02	.1992
.05	.3150
.1	.4382
.2	.6066
.3	.7266
.4	.8198

[a] Exact: 1.00501.

Sonic line	
x/R_s	r/R_s
0.0049	0.0988
.0101	.1288
.0150	.1505
.0254	.1985
.0451	.2720
.0792	.3673
.1200	.4539

Body			
n	x/R_s	r/R_s	p_b
0	0.00855	0	[a]1.0050
2	.00995	.0520	1.0013
4	.01618	.1214	.9848
6	.0275	.1908	.9553
8	.0440	.2600	.9129
10	.0660	.3292	.8586
12	.0937	.3982	.7932
14	.1276	.4670	.7162
16	.1684	.5354	.6293
18	.2168	.6033	.5316

Case 196: Sphere at $M=2$, $\gamma=5/3$

Shock	
x/R_s	r/R_s
0	0
.02	.2001
.05	.3165
.1	.4481
.2	.6350
.3	.7792
.4	.9016

[a] Exact: 0.9518.

Sonic line	
x/R_s	r/R_s
0.1701	0.5852
.2134	.5678
.2451	.5342
.2692	.4923
.2888	.4471
.3050	.4003
.3173	.3508

Body			
n	x/R_s	r/R_s	p_b
0	0.1921	0	[a]0.949
2	.1934	.0352	.944
4	.1994	.0820	.921
6	.2102	.1282	.880
8	.2258	.1738	.823
10	.2464	.2182	.751
12	.2720	.2612	.659
14	.3029	.3022	.553
16	.3399	.3402	.390
17	.3621	.3569	.353

Case 194: Sphere at $M=1.2$, $\gamma=5/3$

Shock	
x/R_s	r/R_s
0	0
.005	.1004
.02	.2033
.035	.2722
.05	.3291
.07	.3953
1	.4829
.15	.6121

Sonic line [a]	
x/R_s	r/R_s
0.1453	0.6005
.2116	.5106
.2255	.3776
.2323	.2728
.2429	.1998
.2550	.1465

Body			
n	x/R_s	r/R_s	p_b
0	0.2065	0	[b]1.118
2	.2082	.0250	1.100
4	.2161	.0577	1.025
6	.2302	.0890	.850
8	.2508	.1179	.648
10	.2794	.1422	.306
11	.3007	.1490	------

[a] First 5 values from supplementary case 246.
[b] Exact: 1.1029.

Case 197: Sphere at $M=3$, $\gamma=7/5$

Shock	
x/R_s	r/R_s
0	0
.02	.1998
.05	.3154
.1	.4448
.2	.6255
.3	.7617
.4	.8745
.5	.9721

[a] Exact: 0.9115.

Sonic line	
x/R_s	r/R_s
0.1460	0.5361
.1946	.5411
.2344	.5314
.2665	.5107
.2918	.4814
.3116	.4459
.3265	.4050
.3374	.3600

Body			
n	x/R_s	r/R_s	p_b
0	0.1645	0	[a]0.912
2	.1661	.0432	.906
4	.1733	.1006	.883
6	.1863	.1575	.838
8	.2053	.2137	.780
10	.2303	.2687	.708
12	.2615	.3223	.623
14	.2995	.3738	.524
16	.3450	.4219	.389
18	.4030	.4622	-----

Case 195: Sphere at $M=1.5$, $\gamma=5/3$

Shock	
x/R_s	r/R_s
0	0
.02	.2007
.05	.3191
.10	.4553
.15	.5625
.2	.6551
.3	.8159
.4	.9575

Sonic line [a]	
x/R_s	r/R_s
0.1731	0.6067
.2178	.5485
.2453	.4740
.2656	.3997
.2830	.3319
.2994	.2722
.3139	.2181

Body			
n	x/R_s	r/R_s	p_b
0	0.2150	0	[b]1.021
2	.2161	.0274	1.015
4	.2212	.0638	.988
6	.2304	.0997	.941
8	.2436	.1348	.853
10	.2610	.1688	.769
12	.2827	.2012	.663
14	.3090	.2314	.523
16	.3416	.2578	------

[a] First 6 values from supplementary cases 247 and 234.
[b] Exact: 1.0134.

Case 198: Sphere at $M=4$, $\gamma=5/3$

Shock	
x/R_s	r/R_s
0	0
.02	.1996
.05	.3148
.1	.4433
.2	.6213
.3	.7540
.4	.8626
.5	.9552

[a] Exact: 0.8981.

Sonic line	
x/R_s	r/R_s
0.1328	0.5093
.1794	.5221
.2190	.5217
.2522	.5112
.2792	.4918
.3005	.4651
.3171	.4327
.3305	.3967

Body			
n	x/R_s	r/R_s	p_b
0	0.1528	0	[a]0.896
2	.1544	.0440	.891
4	.1613	.1025	.869
6	.1738	.1606	.831
8	.1919	.2181	.778
10	.2159	.2748	.711
12	.2459	.3301	.631
14	.2826	.3837	.538
16	.3266	.4345	.418
18	.3812	.4795	-----

TABLE IV.—GEOMETRY AND PRESSURE DATA FOR SPHERES AND PARABOLOIDS—Concluded

Case 199: Sphere at $M=6$, $\gamma=5/3$

Shock	
x/R_s	r/R_s
0	0
.02	.1996
.05	.3145
.1	.4424
.2	.6187
.3	.7492
.4	.8551
.5	.9447

[a] Exact: 0.8887.

Sonic line	
x/R_s	r/R_s
0.1228	0.4891
.1689	.5072
.2092	.5132
.2439	.5095
.2737	.4984

Body			
n	x/R_s	r/R_s	p_b
0	0.1437	0	[a]0.887
2	.1448	.0382	.884
4	.1497	.0691	.869
6	.1586	.1398	.842
8	.1715	.1901	.804
10	.1885	.2400	.756
12	.2098	.2893	.699
14	.2355	.3377	.632
16	.2659	.3850	.557
18	.3016	.4306	.464
19	.3218	.4524	.389

Case 200: Sphere at $M=10$, $\gamma=5/3$

Shock	
x/R_s	r/R_s
0	0
.02	.1995
.05	.3144
.1	.4420
.2	.6177
.3	.7474
.4	.8523
.5	.9407

[a] Exact: 0.8840.

Sonic line	
x/R_s	r/R_s
0.1177	0.4785
.1651	.5000
.2069	.5092
.2429	.5077
.2724	.4963
.2953	.4755
.3149	.4508

Body			
n	x/R_s	r/R_s	p_b
0	0.1388	0	[a]0.883
2	.1400	.0410	.879
4	.1455	.0957	.863
6	.1555	.1501	.833
8	.1700	.2042	.792
10	.1891	.2577	.738
12	.2132	.3105	.675
14	.2423	.3624	.602
16	.2770	.4128	.518
18	.3180	.4610	.411
19	.3410	.4840	.323

Case 201: Sphere at $M=\infty$, $\gamma=5/3$

Shock	
x/R_s	r/R_s
0	0
.02	.1995
.05	.3144
.1	.4419
.2	.6174
.3	.7468
.4	.8514
.5	.9394

[a] Exact: 0.8813.

Sonic line	
x/R_s	r/R_s
0.1150	0.4730
.1631	.4964
.2060	.5076
.2427	.5074
.2729	.4970
.2964	.4771
.3145	.4501

Body			
n	x/R_s	r/R_s	p_b
0	0.1358	0	[a]0.880
2	.1373	.0451	.876
4	.1439	.1050	.856
6	.1557	.1647	.822
8	.1730	.2240	.773
10	.1959	.2826	.711
12	.2247	.3402	.641
14	.2599	.3965	.553
16	.3021	.4507	.451
18	.3533	.5009	.285

U.S. GOVERNMENT PRINTING OFFICE : 1961—O-608307